

Review

Not peer-reviewed version

Review of Foam with Novel CO₂-Soluble Surfactants for Improved Mobility Control in Tight Oil Reservoirs

[Fajun Zhao](#)*, [Mingze Sun](#), Yong Liu, Wenjing Sun, Qinyuan Guo, [Zian Yang](#), Changjiang Zhang, Meng Li

Posted Date: 21 October 2024

doi: 10.20944/preprints202410.1588.v1

Keywords: foam; tight oil reservoirs; CO₂ foam; CO₂ soluble surfactants; mobility control



Preprints.org is a free multidisciplinary platform providing preprint service that is dedicated to making early versions of research outputs permanently available and citable. Preprints posted at Preprints.org appear in Web of Science, Crossref, Google Scholar, Scilit, Europe PMC.

Copyright: This open access article is published under a Creative Commons CC BY 4.0 license, which permit the free download, distribution, and reuse, provided that the author and preprint are cited in any reuse.

Review

Review of Foam with Novel CO₂-Soluble Surfactants for Improved Mobility Control in Tight Oil Reservoirs

Fajun Zhao ^{1,*}, Mingze Sun ¹, Yong Liu ^{2,3}, Wenjing Sun ^{2,3}, Qinyuan Guo ¹, Zian Yang ¹, Changjiang Zhang ¹ and Meng Li¹

¹ Key Laboratory of Enhanced Oil Recovery of Education Ministry, Northeast Petroleum University, Daqing 163318, Heilongjiang, China

² Heilongjiang Provincial Key Laboratory of Reservoir Physics & Fluid Mechanics in Porous Medium, Daqing 163712, China

³ National Key Laboratory for Multi-resource Collaborated Green Development of Continentals Shale Oil, Daqing 163712, China

* Correspondence: fajzhao@126.com

Abstract: CO₂-soluble surfactant foam systems have gained significant attention for their potential to enhance oil recovery, particularly in tight oil reservoirs where conventional water-soluble surfactants face challenges such as poor injectability and high reservoir sensitivity. This review provides a comprehensive explanation of the basic theory of CO₂-soluble surfactant foam, its mechanism in enhanced oil recovery (EOR), and the classification and application of various CO₂-soluble surfactants. The application of these surfactants in tight oil reservoirs, where low permeability and high water sensitivity limit traditional methods, is highlighted as a promising solution to improve CO₂ mobility control and increase oil recovery. The mechanism of enhanced oil recovery by CO₂-soluble surfactant foam involves the effective reduction of CO₂ fluidity, the decrease in oil-gas flow ratio, and the stabilization of the displacement front. Foam plays a vital role in mitigating the issues of channeling and gravity separation often caused by simple CO₂ injection. The reduction in gas fluidity can be attributed to the increase in apparent viscosity and trapped gas fraction. Future research should prioritize the development of more efficient and environmentally-friendly CO₂-soluble surfactants. It is essential to further explore the advantages and challenges associated with their practical applications in order to maximize their potential impact.

Keywords: foam; tight oil reservoirs; CO₂ foam; CO₂ soluble surfactants; mobility control

Introduction

Carbon capture, utilization, and storage (CCUS) technology is a new development direction for carbon capture and storage (CCS) technology. CCUS captures and purifies CO₂ released during the manufacturing process and then reintroduces it into the new production process for recycling. Notably, CCUS is more cost effective and environmentally friendly than CCS. CO₂ injection has been an important and widely used enhanced oil recovery (EOR) technology for the past 50 years^[1,2]. Because oil reservoirs are well-sealed, underground gas storage for long-term CO₂ retention^[3] (Figure 1), CO₂ injection can achieve social benefits while increasing economic benefits. However, in tight oil reservoirs characterized by low permeability and high water sensitivity, conventional CO₂ flooding often faces challenges such as viscous fingering, gravity override, and gas channeling, which limit its effectiveness. CO₂-soluble surfactants present a promising solution for these challenges. The impact of reservoir heterogeneity on foam propagation and stability has been extensively studied, highlighting challenges in achieving uniform displacement in porous media^[4,5]. Unlike water-soluble surfactants, CO₂-soluble surfactants can dissolve directly in the CO₂ phase and form stable foams upon contact with reservoir water, improving sweep efficiency and mitigating the issues caused by reservoir heterogeneity. The application of these surfactants in tight oil reservoirs has the potential

to significantly enhance oil recovery by improving CO₂ mobility control and reducing gas flow instabilities. In addition, CO₂ injection is one of the most effective means of CO₂ utilization and storage. Furthermore, the effect of CO₂ EOR depends on the oil displacement efficiency and swept volume of CO₂ in the reservoir. Viscous fingering, gravity overshooting, and gas channeling will occur in the middle or late stages of reservoir development due to the low density, low viscosity of CO₂, and formation heterogeneity. Because these phenomena have a significant effect on the efficacy of CO₂ injection for EOR^[6], the effective mobility control of CO₂ is the key to its efficient utilization.

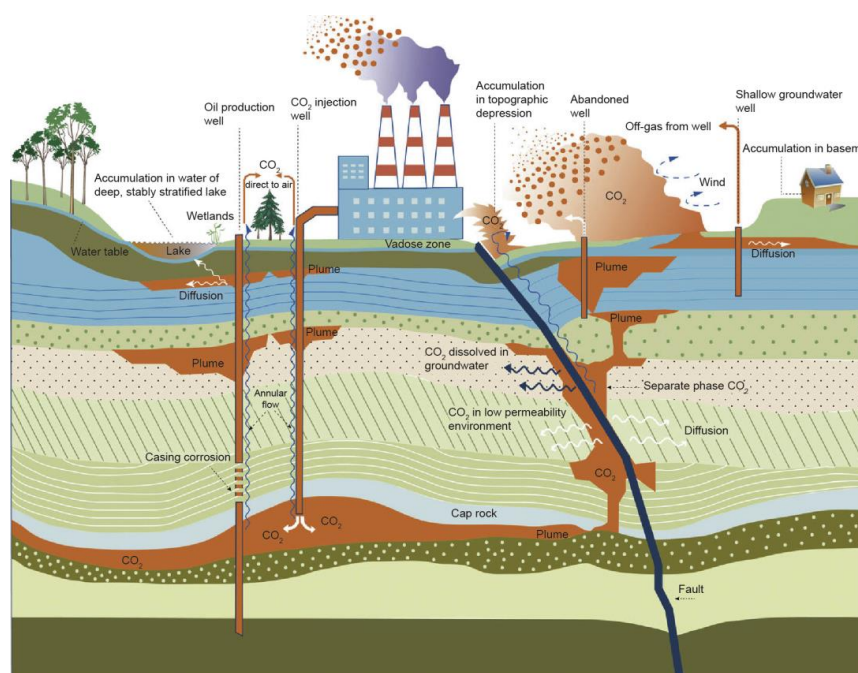


Figure 1. Mechanism and effect of CO₂ leakage in geological buried sites ^[7].

Owing to its characteristics of “plugging large holes instead of small ones and plugging water instead of oil,” foam flooding can effectively control gas flow and improve displacement efficiency^[7] (Figure 2). It can also improve formation heterogeneity and inhibit gas channeling efficiently. Therefore, greater attention has been given to CO₂ foam flooding technology, which has many advantages in flow control^[7–19]. CO₂ foam flooding functions by forming a multiphase dispersion system in which a surfactant aids the liquid film in dispersing CO₂ in the liquid phase. Therefore, foam can effectively improve displacement front fingering and gas channeling by reducing the mobility ratio of CO₂ and crude oil^[8,9]. Recent studies have made significant strides in CO₂-soluble surfactant technology, particularly focusing on surfactants that enhance foam stability and oil displacement in harsh reservoir conditions. For example, Li et al.^[10] explored new amphiphilic surfactants that exhibited superior stability under high temperature and salinity conditions, extending foam half-life by over 30% compared to traditional surfactants. Similarly, recent work by Liang et al.^[11] demonstrated that adding certain alcohol agents significantly enhances surfactant solubility in supercritical CO₂, improving injectability in low-permeability reservoirs. These advancements highlight the growing importance of optimizing CO₂-soluble surfactants for enhanced oil recovery in unconventional reservoirs. Hosseini's work on the utilization of CO₂ with polyelectrolyte complex nanoparticles and surfactants offers significant insights into environmentally friendly oil recovery methods, which is crucial for modern enhanced oil recovery (EOR) practices^[12].

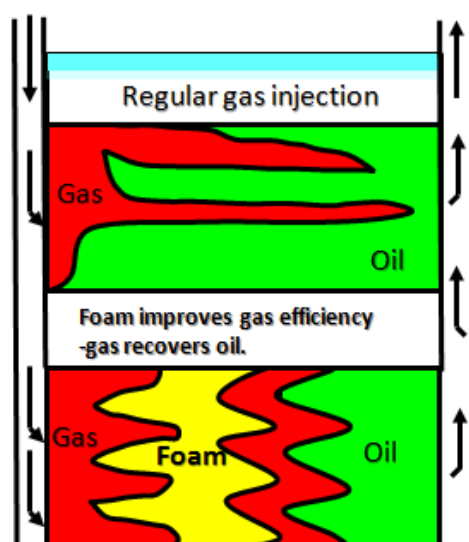


Figure 2. Improvement of gas transport in porous media by foam.

Considering foam technology's progressive growth, some key barriers to the implementation of conventional CO₂ foam are as follows: (1) The injection of conventional foam inhibits part of the CO₂ flooding effect due to the water-soluble surfactant slug phenomenon, which hinders the CO₂–crude oil contact; (2) The regeneration ability is limited because CO₂ is separated from surfactant by gravity after foam burst^[21]; (3) When exploiting unconventional reservoirs, such as low-permeability and tight oil reservoirs, high water sensitivity, poor water absorption capacity of injection wells, high injection pressure, and even no water injection can occur. Because the permeability of unconventional reservoirs is usually much lower than that of conventional reservoirs. Low permeability means greater resistance to fluid flow, and the function of surfactants in reducing oil-water interfacial tension and promoting droplet movement is also limited. In addition, some unconventional oil reservoirs have water sensitivity, which means that when clay minerals in the reservoir come into contact with water, they may expand or move, further blocking pores and reducing permeability, making injection more difficult. Because the surfactant aqueous solution cannot be injected, CO₂ foam technology may not be used in unconventional reservoirs ^[22]. The limitation of aqueous phase injection caused by low permeability and water sensitivity requires higher pressure to inject foam formed by CO₂ and surfactant. At the same time, the temperature of unconventional oil reservoirs may be much higher than that of conventional oil reservoirs. Therefore, under the environment of high temperature and high pressure, the solubility of CO₂ increases, which may affect the stability of foam, thus affecting its oil displacement ability. CO₂/foam technology will also affect the reservoir environment. The problem of water sensitivity may aggravate the plugging of rock pores, further reduce the permeability and hinder the effective migration of foam. The use of surfactant may affect the microbial ecosystem in the reservoir, or pollute the surface water and groundwater after the foam bursts. To overcome these limitations, it may be necessary to develop surfactants that are more resistant to high temperature and pressure, improve foam generation and injection technology, and optimize operating parameters. As an alternative, a solubility surfactant-based CO₂ foam mobility control system is therefore proposed. Some specific surfactants can dissolve in supercritical CO₂, a green solvent, and can be directly injected into the reservoir. After the surfactant contacts with water in the reservoir, a CO₂ foam or emulsion forms *in situ* to control the CO₂ flow rate. The stability and quality of foam can be controlled by adjusting the concentration of injected surfactant and the injection rate of carbon dioxide. In unconventional oil reservoirs, low permeability and water sensitivity are common challenges that affect the efficiency of oil displacement. The use of CO₂-soluble surfactants can alleviate the unfavorable effects of these problems to some extent. CO₂-soluble surfactants have high solubility in supercritical CO₂ and can enhance the interaction between CO₂

and crude oil, control the mobility of CO₂, and thus improve the CO₂ oil displacement effect, showing great potential for enhancing oil recovery.

Gas-soluble surfactants have comparable displacement performance to water-soluble surfactants. Utilizing CO₂ as the injection carrier enhances surfactant injectability in low-permeability reservoirs [24,25]. CO₂-soluble surfactants offer several key advantages when applied to tight hydrocarbon reservoirs. Firstly, their ability to dissolve directly in CO₂ without the need for an aqueous phase makes them highly suitable for low-permeability reservoirs where water injection is not feasible or is limited by high water sensitivity. This significantly reduces the risk of formation damage caused by water blockages, which is a common issue in tight oil reservoirs. Additionally, the ability of CO₂-soluble surfactants to form stable foams under high-pressure and high-temperature conditions enhances their effectiveness in controlling CO₂ mobility, reducing gas channeling, and improving sweep efficiency. Their injectability in supercritical CO₂ allows for deeper penetration into the reservoir, which is critical for improving oil recovery in heterogeneous formations. Furthermore, CO₂-soluble surfactants have shown better regeneration capabilities after foam rupture, which extends the foam stability time and improves the overall oil recovery process. In addition, the surfactant carried by the CO₂ phase favors foam regeneration after foam bursting, hence extending the foam's stability time. When the foam breaks, the molecular structure of the surfactant can be rearranged, and a stable liquid film can be formed at the edge of the broken foam, which enables the foam to maintain its integrity, thus maintaining the structural stability. Notably, CO₂ is a nonpolar molecule, as its dipole moment is zero. Because CO₂ has an extremely low dielectric constant and van der Waals force, its solubility in high molecular weight molecules is extremely low [24,25]. For low concentrations, surfactant concentration positively correlates with foam performance. At low concentrations, with the increase of surfactant concentration, more surfactant molecules can be adsorbed on the air liquid interface, reducing the surface tension of foam film, reducing the coalescence and rupture between foam, and enhancing the stability of foam. The surfactant solubility in CO₂ plays a crucial role in the foaming effect of gas-soluble surfactants. Furthermore, researchers have developed many gas-soluble surfactants and agents based on CO₂ characteristics. These surfactants must be separated due to their differences. Meanwhile, this review would benefit from a summary of the gas-soluble surfactant dissolution mechanism, agent solubilization mechanism, foam formation mechanism in porous media, mobility model, and EOR mechanism of CO₂ foam.

Despite these advantages, several challenges remain in the utilization of CO₂-soluble surfactants in tight hydrocarbon reservoirs. One of the primary challenges is their chemical stability under extreme reservoir conditions, including high temperatures, pressures, and salinity levels, which may lead to surfactant degradation or reduced effectiveness over time. Furthermore, the solubility of certain CO₂-soluble surfactants can vary significantly depending on the specific reservoir conditions, which may affect foam generation and stability. Another challenge is the cost associated with synthesizing and scaling up these specialized surfactants, particularly for large-scale field applications. Additionally, there are operational challenges related to ensuring uniform distribution of the surfactant within the reservoir, especially in highly heterogeneous formations. Addressing these challenges will require further research into surfactant formulations, cost-effective production methods, and more advanced injection techniques to optimize the performance of CO₂-soluble surfactants in tight oil reservoirs.

Based on the aforementioned issues, this paper is divided into three sections to discuss recent advances in CO₂ gas-soluble surfactant research. The first section centers on the composition, classification, and experiment of CO₂ foam system; the second section explores the basic concept of CO₂ foam and the EOR mechanism; and the third section focuses on the classification of and discussion on gas-soluble surfactants developed from field and laboratory experiments. Finally, the CO₂ foam mechanism and development direction of gas-soluble surfactants are summarized and prospected as a reference and inspiration for future research.

To provide a clear overview of the scope of this article, a flow chart summarizing the main research areas and findings is presented below. This chart outlines the key components of the study,

including the development of CO₂-soluble surfactants, their evaluation through experimental methods, their application in tight oil reservoirs, and potential future research directions.

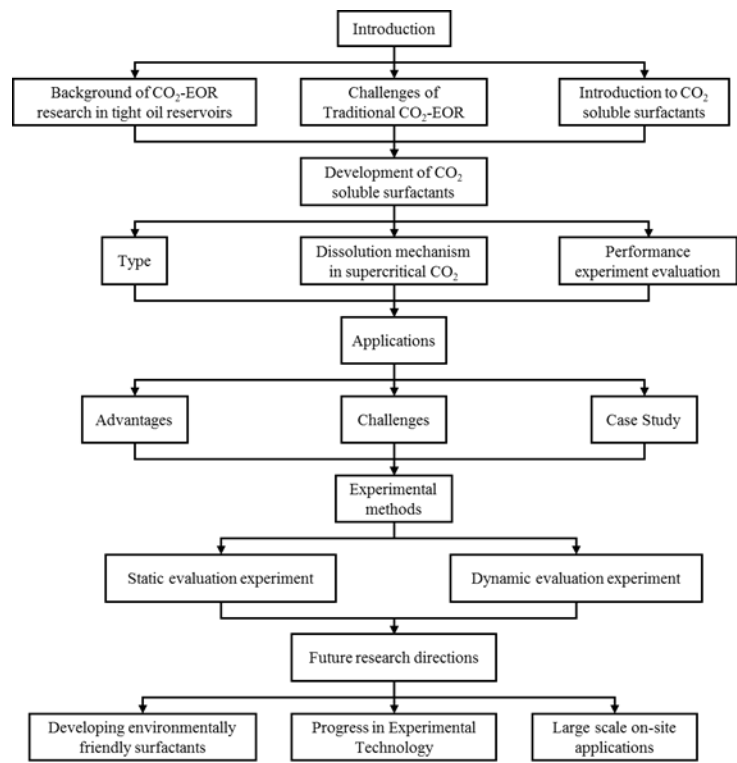


Figure 3. Scope of the review.

1. CO₂-Soluble Surfactant Foam System

1.1. The Dissolution Method of the System

Bernard et al. [29] were the first to propose the concept of surfactant dissolution in CO₂. Since then, the injection method's main research focus has been surfactant dissolution in CO₂ and its simultaneous injection, as experimental research and field tests have demonstrated the great potential of this method. The dissolution modes of surfactant in CO₂ can be divided into two types: CO₂ + surfactant system (+agents) and CO₂ + surfactant + water (+ agents). That is, the surfactant dissolves in CO₂ or trace water to form a microemulsion in supercritical CO₂. Table 1 lists the application progress of the two CO₂ foam systems in the oil field or laboratory experiments.

1.1.1. CO₂ + Gas-Soluble Surfactants (+ Agents)

During CO₂ flooding or CO₂ huff and puff, gas-soluble surfactants produce foam or emulsion *in situ* after contact with formation water, which can increase the apparent viscosity of the CO₂ gas phase, control CO₂ fluidity, and plug the large channel. Bernard et al.[29] studied the use of supercritical CO₂ dissolution capacity to transport surfactants into the reservoir to generate foam. The results showed that adding surfactants can control CO₂ in foam formation and improve oil recovery while reducing CO₂ concentration. Through laboratory experiments, Xue et al. [23] demonstrated the excellent thermal and chemical stability of two surfactants by measuring parameters such as water phase stability, static and dynamic adsorption, CO₂ solubility, interfacial tension, foam size, and foam viscosity. The two surfactants reduced the adsorption of the sandstone reservoir. They also found that high temperature and CO₂ dilution by methane reduced foam stability. Foad et al. [30] conducted huff and puff experiments on the CO₂-surfactant system at 80°C, 4000 psi. The experiment used a non-ionic surfactant N-NP10c, which belongs to the alkylphenol polyoxyethylene ether class. After eight cycles, approximately 75% of crude oil was extracted. N-NP-

10c was 0.15% soluble in supercritical CO₂ without agents but was 1.76% soluble with agents, an increase of 11 times^[25,31]. Bi et al. ^[31] found that adding ethylene glycol can improve the solubility of surfactants with high polarity in ethanol. Nonionic surfactants can exhibit relatively high solubility in supercritical CO₂ by the action of alcohol agents. Liu et al. ^[32] found that bis(2-ethylhexyl) sulfosuccinate sodium salt (AOT) can be dissolved in supercritical CO₂ with less F-pentanol than ethanol and 1-pentanol because F-pentanol has a “CO₂-philic” fluorinated alkane chain.

1.1.2. CO₂ + Gas-Soluble Surfactant + Water (+ Agents)

Based on CO₂ + gas-soluble surfactant, researchers have improved and proposed the CO₂ + gas-soluble surfactant + water + (agent) system in which the addition of trace water can form nanoscale aggregates in supercritical CO₂. Some hydrophilic, extremely polar, or macromolecular solutes can be transported within the aggregates' core. Since Johnston et al. ^[33] first confirmed the existence of supercritical CO₂ microemulsion, extensive research has been conducted on this subject. Zhang Chao^[28] found that as the ethanol concentration in a supercritical CO₂ microemulsion system increased, the foaming volume increased, then decreased, but remained greater than that without ethanol. The rise in foam half-life with increasing ethanol concentration indicated that ethanol addition facilitated the formation of stable CO₂ foam by AOT. Cui et al.^[34] demonstrated that the tendency of the cloud point pressure of a supercritical CO₂ microemulsion system to vary with temperature differs depending on the water content. The cloud point pressure of the supercritical CO₂ microemulsion drops with increasing surfactant AOT content before increasing. Notably, the relationship between AOT content and cloud point pressure is consistent at various temperatures. Some researchers found that^[35] alkyl chain alcohols can greatly reduce the cloud point pressure, and the smaller the molecular weight of the alcohol, the better the effect. When the temperature increases, the cloud point pressure increases, which then decreases when the alcohol concentration increases.

The mechanism of surfactant dissolution in CO₂ can be divided into two categories: (1) the surfactant can directly dissolve in the CO₂ system and (2) the addition of surfactant and a small amount of water to CO₂ to form a supercritical CO₂ microemulsion system containing polar microwaters. This system is thermodynamically stable, isotropic, and optically transparent. Furthermore, the simple use of a CO₂ + gas-soluble surfactant system can clog the channel and improve oil recovery efficiency by forming foam *in situ* with formation water. However, due to the low solubility of CO₂ in gas-soluble surfactants, the foam performance of the surfactant is limited, hence limiting the flooding effect. Adding alcohol agents can effectively enhance the CO₂ solubility of a gas-soluble surfactant while promoting the formation of a supercritical CO₂ microemulsion. In the past, increasing the solubility of supercritical CO₂ has primarily been aimed at extracting hydrophilic, highly polar, or macromolecular solutes, such as metal ions and proteins, for various applications in chemical engineering and materials science. Therefore, the second method is often used to form supercritical CO₂ microemulsion to improve supercritical CO₂ solubility.

Table 1. Progress of two types of CO₂ foam systems in the field or experiment.

Surfactant	Additives	Research Focus	Results	Conditions	References
AMPHOAM, LDMAA	—	Foam stability at high temperatures and salinity, effect of methane dilution	Good thermal and chemical stability. High temperatures and methane dilution reduce foam stability.	120°C, High salinity	[23]
SURFONIC® N-100,	—	Surfactant effect on rock wettability	Enhanced rock wettability and	80°C, 2000-5000 LBS/Sq	[30]

SURFONIC® TDA-9		and CO ₂ huff-and-puff performance	improved recovery (75%)		
N-P series, ABS, A-S-12, N-NP-7c/9c	Ethanol, Glycol	Solubility and extraction performance of surfactants with CO ₂	N-P-12 with additives showed the highest solubility, stable foam at 125°C	125°C	[31]
AOT	Ethanol, 1-pentanol	Solubility in supercritical CO ₂ under different additives and pressures	F-pentanol enhanced solubility and lowered cloud point pressure	52.2°C, 35 MPa	[32]
AOT, SDS, C8PnEm, C12EmPn	—	Comprehensive performance screening of surfactants and effect of pressure and temperature	Optimal concentration at 0.5%. Stability varies with temperature and pressure.	40°C, 15-50 MPa	[28]
AOT	Ethanol	Effect of temperature, water content, and AOT concentration on cloud point pressure of CO ₂ microemulsions	Cloud point pressure changes with AOT content and temperature.	45°C, 19 MPa	[34]
Ls-54	Alcohols (various)	Effect of different alcohols on the phase behavior of CO ₂ -containing surfactants	Smaller molecular weight alcohols lower cloud point pressure, temp increases pressure.	308.2K and 318.2K, 13.67-22.87 MPa	[35]

1.2. Evaluation of the System

The CO₂ foam research based on gas-soluble surfactants is not yet mature. Existing research mainly focuses on indoor experimental and theoretical studies, and only a few field tests exist. The Petroleum Engineering Technology Research Institute of Shengli Oilfield conducted the first on-site test on the application of carbon dioxide gas soluble foaming agent in China to address the occurrence of gas channeling in the high 89-1 block carbon dioxide flooding reservoir of Chunliang Oil Production Plant. The test successfully formed a carbon dioxide foam underground, effectively blocked the underground channeling channel, and improved the spread area of CO₂ and oil recovery. According to these studies, gas-soluble CO₂ foam is mainly injected in two ways: (1) through

water-alternating-gas injection, which entails dissolving the surfactant in the gas phase and injecting it into the formation with the gas phase slug^[36]. (2) The second approach entails dissolving the surfactant in CO₂ and injecting the mixture into the formation continuously. During the injection process, the liquid phase is not injected. Foam generation results from the interaction between the CO₂-carried surfactant and water phase in the formation^[24].

The laboratory study of CO₂ foam mainly includes static and dynamic experiments. Static experiments are always used to investigate the foaming ability and foam stability of surfactants. The surfactant's foaming ability was analyzed based on the observed foam volume and half-life. Figure 3(a)^[37] shows the static experimental system, which includes CO₂ gas source, foam solution tank, and PVT reactor. Through the reactor's viewing window, the foam volume and foam half-life can be observed to evaluate the surfactant's foaming ability and foam's stability. Figure 3(b)^[28] depicts the dynamic experimental system, which mainly includes the sand filling model, injection, data reading, production, and auxiliary systems. The injection system mainly comprises CO₂ gas cylinder, dryer, liquefier, booster pump, sampler, and intermediate container.

Notably, the surfactant's interfacial properties must be measured using laboratory experiments to evaluate its performance. Figure 4^[28] depicts the experimental system, which mainly comprises a high temperature and high pressure vessel with a visual window, pressure, and temperature control system, CO₂ injection system, motor drive system, and computer data acquisition system. The system could measure temperatures up to 200°C and pressure up to 20 MPa. The interfacial tension (IFT) between CO₂ and surfactant solution was measured by automatic droplet shape acquisition and analysis using electric heating. In summary, the laboratory foam injection system is generally divided into three parts: CO₂ gas source, sample preparation instrument, and surfactant solution. According to different uses, the laboratory research system can be divided into static experiments (determination of foaming performance and foam thermal stability) and dynamic experiments (determination of foam plugging performance). As a result, depending on the experimental purpose, a suitable experimental system and methodologies must be chosen.

In terms of experimental methods, future research should aim to improve both static and dynamic testing protocols for CO₂-soluble surfactants. Current laboratory methods for testing surfactant foam stability and injectability under high-pressure, high-temperature conditions can be enhanced by incorporating advanced simulation techniques such as molecular dynamics simulations and computational fluid dynamics (CFD) models. These simulations can help predict surfactant behavior before physical experimentation, thereby reducing trial-and-error in the laboratory.

Additionally, high-throughput screening techniques could be developed to accelerate the discovery of new surfactants. This could involve automated systems capable of testing thousands of surfactant formulations under varying conditions of temperature, pressure, salinity, and reservoir heterogeneity, providing rapid feedback on the most promising candidates for further testing. In terms of field testing, mini-pilot tests in controlled environments could offer valuable data on surfactant performance at a fraction of the cost and risk associated with full-scale field trials.

Finally, further improvements in microemulsion and foam generation technologies, such as real-time in-situ monitoring of foam behavior during injection, would allow for better control over foam stability and distribution in the reservoir. Utilizing sensor technologies that can track foam formation and movement within the reservoir could provide valuable insights into optimizing foam injection strategies and improving the overall efficiency of CO₂-EOR processes.

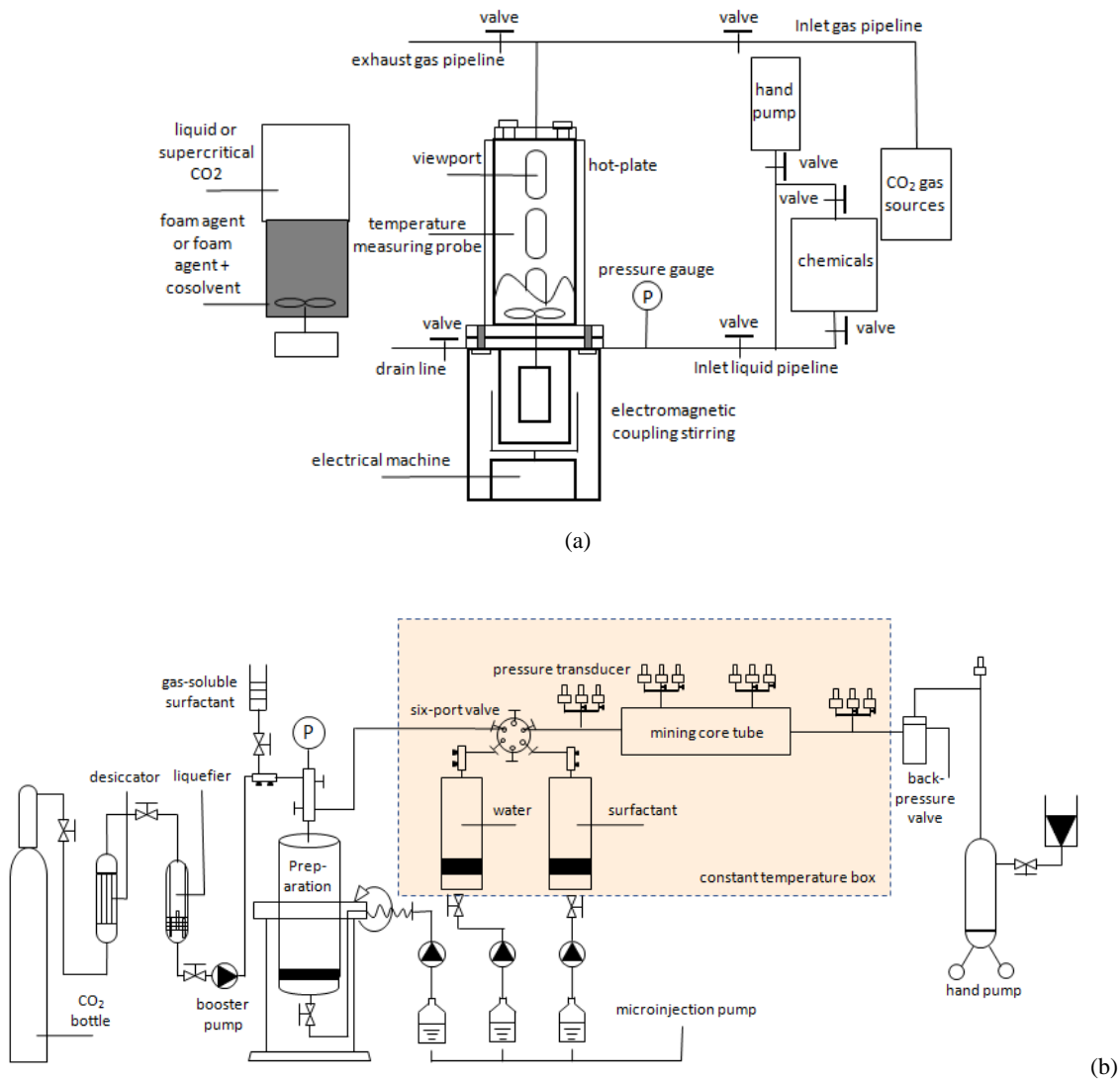


Figure 4. Laboratory experimental study of CO₂ foam system (a) static experiment [34]; (b) dynamic experiment [28]).

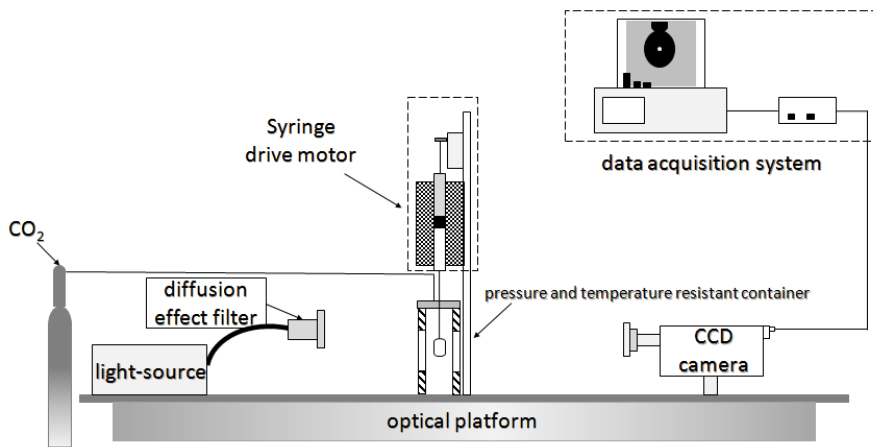


Figure 5. Interface tension experimental device [28].

1.3. CO₂ Foam Performance Evaluation Methods

The dissolution, foaming, and displacement of the CO₂ foam process require a series of evaluation indicators for analysis. To realize a better model for CO₂ foam performance and effectiveness, the program and equation should be adjusted and improved promptly. Table 2 lists the common indices of gas-soluble CO₂ foam laboratory research. Using foam volume (V) (or height) and foam half-life ($t_{1/2}$), the static experimental evaluation method can be used to assess the gas solubility, foaming ability, stability, compatibility, and heat resistance of a surfactant. The macroscopic phase behavior of a surfactant, water, and CO₂ can also be determined based on the cloud point pressure, after which the stability and solubilization performance of the microemulsion can be determined^[28]. Surfactant dissolution in supercritical CO₂ can alternatively be viewed as the mixing of solvent and solute. The solubility parameter and volume fraction of solvent and solute were used to determine the mixing enthalpy, which was then used to calculate the solubility parameter (δ)^[39]. The dynamic experimental evaluation method entails analyzing the foam's plugging ability by measuring the basic pressure difference (ΔP_b) and working pressure difference (ΔP_r) on both sides of the sand-filled pipe to obtain the resistance coefficient (R_f) and residual resistance factor^[28,40,41]. By calculating the residual oil saturation of the core^[42], the oil displacement efficiency (E_D) of the core experiment was obtained^[40]. The evaluation method for improving sweep efficiency entails using a two-dimensional model or double-tube parallel model for the displacement experiment. Gas injection temperature, gas injection rate, oil production rate, cumulative liquid production, cumulative production degree, and water content should be recorded, after which a map of the relationship between the above data and pore volume or experimental time is drawn and analyzed. In addition, the gas-soluble surfactant can effectively reduce the miscible pressure of CO₂ because it forms miscible flooding with crude oil. Therefore, the interface performance must be measured using the hanging drop method to examine the change in miscible pressure^[43].

Foam rheology requires careful consideration of foam quality and gas volume fraction in the total injected fluid. Steady-state foam can be divided into two state intervals: low mass and high mass^[44]. In low-mass regions, shear thinning dominates foam behavior, which can be characterized by an empirical equation, whereas high-mass regions display both shear thinning and shear thickening. The foam behavior in the high-mass area can be analyzed using a model based on the concept of "limit capillary pressure"^[44–46]. The foam strength increases as the foam mass increases in the low-mass areas. The foam strength peaks at the junction between the high and low foam masses and decreases as the foam mass increases in the high-mass areas. This trend is due to the different behavior of foams in these regions. Assume that the foam size is constant in the low-mass areas; then, as the foam quality increases, the number and apparent viscosity of the foams increase^[47]. In addition, a varying range of foam sizes exists^[48]. Most current research on foam quality is concentrated in the 40%–95%–range because fluidity reduction is infeasible due to foam's instability outside this range^[49]. In addition, advanced models that simulate foam behavior in porous media have also considered the effects of nanoparticle-enhanced stability, which allows for more accurate predictions of foam performance in the field^[50,51].

Because it cannot be measured directly, foam viscosity is usually expressed as foam fluidity or apparent viscosity. Foam fluidity is defined as the ratio of effective permeability to apparent viscosity. If the gas phase is continuous, the foam will only reduce the cross-sectional area through which the gas flows, resulting in a drop in relative permeability. If the gas phase is discontinuous, the relative permeability decreases and the foam also has a high apparent viscosity, which reduces the gas fluidity^[52]. Bond et al.^[53] first defined the concept of "foam-reducing gas mobility" and expressed it by MRF (mobility reduction factor). Thereafter, the MRF is commonly used to describe foam-reducing gas mobility. MRF can be calculated using the ratio of foam flooding pressure drop to water/gas flooding pressure drop^[54]. The apparent viscosity of foam in porous media depends on foam size. The smaller the foam, the more lamellae transported through the porous medium and the greater the flow resistance^[55]. Falls et al.^[52] found that if the ratio of foam size to average pore size decreases by two times, the apparent viscosity of the gas increases by an order of magnitude.

In summary, the static and dynamic evaluation methods of CO₂ foam experiments can effectively evaluate most gas-soluble surfactant foams.

Table 2. Evaluation parameters of CO₂ foam laboratory study.

Evaluation index	Definition	Equation	Reference
Foam volume (V)	The space volume occupied by foam at a certain moment	—	[37]
Foam half-life (t _{1/2})	Time taken to reduce the foam volume from the maximum foam volume (V _{max}) to half the volume at a given temperature	—	[38]
Cloud point pressure	Read the pressure at the critical point when the system becomes turbid Proposed based on the regular solution theory, whose value is the	—	[28]
Solubility parameter (δ)	square root of the liquid cohesive energy density, used to characterize the strength of interaction between simple liquid molecules $\Delta H_m = V_m \varphi_1 \varphi_2 (\delta_1 - \delta_2)^2$ (1)		[39]
Basic differential pressure (ΔP _b)	The pressure difference generated at both ends of the core when water and non-condensable gas are injected into the core at the experimental injection rate and gas-liquid ratio.	—	[40]
Working pressure difference (ΔP _r)	Pressure difference at both ends of a foam solution of a certain concentration and a non-condensable gas injected into a core at the same injection rate and gas-liquid ratio as the basic pressure difference measured	—	[40]
Resistance factor (R _f)	At a certain temperature, the ratio of resistance pressure difference (ΔP _r) to basic pressure difference (ΔP _b) $R_f = \frac{\Delta P_r}{\Delta P_b}$ (2)		[41]
Residual resistance factor	Ratio of pressure difference between two ends of subsequent water flooding to that before foam injection after foam injection	—	[28]
Residual oil saturation (S _{or})	Percentage of residual oil in rock pore volume $S_{or} = \frac{W_{or}}{V_p \rho_{oil}}$ (3)		[42]
Displacement efficiency (E _D)	The ratio of produced oil to crude oil in the range of underground displacement $E_D = \frac{\sum_{i=1}^n \frac{W_i}{\rho_{oil}}}{S_{or} V_p} \times 100\%$ (4)		[40]
Interfacial tension	Shrinkage capacity at unit length liquid interface	—	[28]
Foam quality (%)	Gas volume fraction in foams $Foam\ Quality\ (\%) = \frac{gas\ volume}{gas\ volume + liquide\ volume} \times 100$ (5)		[56]
Mobility reduction factor (MRF)	Ratio of foam flooding pressure drop to water/gas flooding pressure drop $MRF = \frac{\left(\frac{\Delta p_{foam\ flood}}{Q_{foam\ flood}}\right)}{\left(\frac{\Delta p_{water/gas\ flood}}{Q_{water/gas\ flood}}\right)}$ (6)		[57]
Apparent foam viscosity (μ _{app})	Ratio of shear stress to shear rate of foam under certain velocity gradient $\mu_{app} = \frac{k}{\mu_t} \cdot \frac{\Delta p}{L}$ (7)		[58]

2. The theory of CO₂-Soluble Surfactant Foam and the EOR Mechanism

2.1. Definition of Foam

Foam is usually defined as a dispersion of gas in a continuous liquid phase^[52,59–61]. A “lamella” separates the gas phase and makes it discontinuous in a liquid film. The lamellae are thin liquid films with interfaces on both sides of the liquid phase (Figure 5)^[65]. In other words, they are thin, free aqueous retention layers surrounded by gas on both sides. The liquid phase usually contains surfactants, which stabilize the lamella via surfactant adsorption at the gas/liquid interface^[60]. Surfactant molecules are generally adsorbed on both sides of the liquid film to stabilize the film. The liquid film thickness is only a few microns or even only a few nanometers. When the film is connected to other lamellae, the area can be expanded to a few square meters^[66]. The liquid phase may also contain macromolecules or solid particles as alternatives to surfactants. As shown in Figure 6^[61], the bottom of the bulk foam structure is the liquid phase and the top is the gas phase. The gas phase separates from the lamellar liquid phase through a two-dimensional interface at the microscopic level.

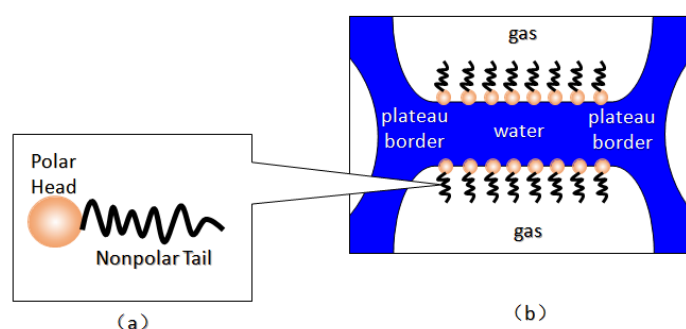


Figure 6. Foam structure in porous media ((a) Surface active molecules; (b) Lamellar structure)^[65].

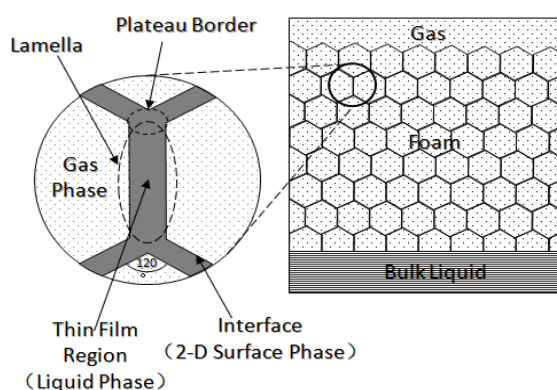


Figure 7. Generalized foam system^[61].

2.2. Surfactant Solubility in CO₂

Because the solubility of gas-soluble surfactant in CO₂ plays a decisive role in its displacement effect, several studies have been conducted in this regard. Rossen et al.^[67] qualitatively determined the solubility of more than 130 commonly used surfactants in supercritical CO₂, including ionic and nonionic surfactants. The results showed that these surfactants were basically insoluble or slightly soluble in supercritical CO₂. Consan et al.^[68] also found that most surfactants are insoluble or slightly soluble in supercritical CO₂. These common surfactants failed to dissolve in CO₂ because the interaction between the hydrophobic chains of surfactants was stronger than that between the CO₂ and hydrophobic chains. To address this issue, Hoefling et al.^[69] improved the surfactant by introducing functional groups with low polarity, low solubility parameters, and Lewis bases into the CO₂-philic tail chain. Gas-soluble surfactants should meet the following three conditions^[70–73]: (1) The hydrophobic tail chain with the CO₂-philic functional group must be able to improve surfactant compatibility with CO₂ and must have a lower cohesive energy density to reduce the interaction

among surfactants. (2) Surfactant hydrophilic-linked double-tail chains or branched chains on the hydrophobic tail chain should be able to increase steric hindrance. (3) Greater flexibility of the surfactant molecular chain should translate into higher surfactant solubility in CO₂. The glass transition temperature primarily determines the flexibility of the molecular chains. The flexibility of a molecular chain increases as its glass transition temperature decreases. External factors also influence solubility. In general, while solubility increases with increasing pressure, it decreases as temperature rises.

Surfactants can dissolve directly in CO₂ when a small amount of water is added to form a supercritical CO₂ microemulsion system. Supercritical CO₂ microemulsion is a water-in-CO₂ (W/C) emulsion. The continuous phase is supercritical CO₂, and water is the discontinuous phase. This microemulsion usually comprises supercritical CO₂, surfactant, and water. Figure 7^[34] shows the structure diagram of the supercritical CO₂ microemulsion and its formation process. The surfactant hydrophilic chain is inward, forming a nanoscale polar “micro pool” that can hold water molecules in the CO₂ continuous phase. The surfactant hydrophobic CO₂ tail chain extends in the CO₂ continuous phase. The droplet size of the microemulsion is generally ten to several hundred nanometers^[74–76]. The ratio of solubilized water to the number of surfactant molecules in the microemulsion (denoted as W_0) reflects the size of the microemulsion water content—an important parameter that reflects the microemulsion characteristics.

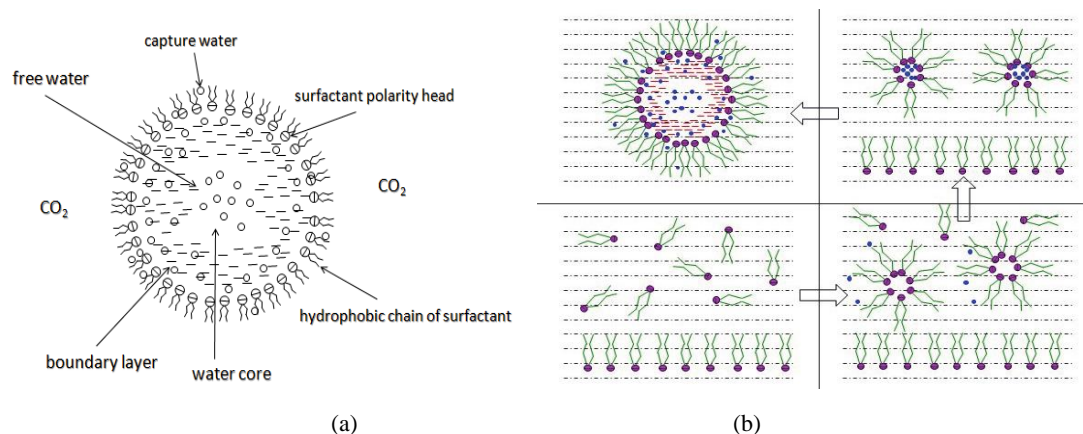


Figure 8. (a) Reverse micelle structure in supercritical CO₂ microemulsion; (b) Process of surfactant formation solubilization micelle in supercritical CO₂ ^[34].

Supercritical CO₂ microemulsions have the following main characteristics^[77,78]: (1) Supercritical CO₂ microemulsion is a thermodynamically stable system. Macroscopically, all directions are uniform, clear, transparent, and have a good dispersion. (2) The aqueous phase of the microemulsion core has two states: free water and bound water. The bound water closely interacts with the surfactant hydrophilic chain in the microemulsion, making the bound water close to the polar surface of the microemulsion core. Free water exists at the center of the microemulsion core, and its water molecules are highly hydrogen-bonded. (3) The continuous phase of CO₂ has very low viscosity and interfacial tension, and the specific surface area of the water core of the microemulsion is large, indicating that a very large contact area exists between the continuous phase CO₂ and the dispersed phase. (4) Although the continuous phase of the supercritical CO₂ microemulsion is nonpolar CO₂, the aqueous phase of its core is polar. Therefore, supercritical CO₂ can solubilize fat-soluble organic compounds and water-soluble polar compounds but cannot dissolve high-ion compounds^[79]. The ability of surfactants to form microemulsions in supercritical CO₂ is closely related to their molecular structure^[80]. Eq. (8) is the ratio of the cohesive energy of the surfactant functional groups at the interface of the microemulsion aggregates. It can be used to predict whether a surfactant can form a microemulsion in supercritical CO₂ or water.

$$R = \frac{A_{co} - A_{oo} - A_{ll}}{A_{cw} - A_{ww} - A_{hh}}, \quad (8)$$

where A_{co} represents the interaction between the CO₂-philic group in the surfactant and CO₂. A_{oo} represents the CO₂-CO₂ interaction. A_{ll} represents the interaction between the CO₂-philic groups in the surfactant. A_{cw} represents the interaction between the hydrophilic groups and water in the surfactant. A_{ww} represents the interaction between water molecules. A_{hh} represents the interaction between the hydrophilic groups in the surfactant.

This equation essentially compares the cohesive energy of surfactant molecules in the CO₂ phase with that in the water phase. A higher value of RRR indicates that the surfactant is more likely to dissolve in supercritical CO₂, while a lower value suggests that the surfactant will more readily dissolve in water or other polar solvents.

The practical use of Eq. (8) lies in its ability to provide a theoretical basis for predicting the solubility of different surfactant formulations in supercritical CO₂. By calculating the cohesive energy parameters based on molecular dynamics simulations or experimental data, researchers can estimate the likelihood of a surfactant dissolving in CO₂ without the need for extensive trial-and-error experimentation. This can save significant time and resources in the development of new CO₂-soluble surfactants.

For example, if A_{co} (the interaction between the CO₂-philic group and CO₂) is much larger than A_{cw} (the interaction between the hydrophilic group and water), the surfactant is likely to be more soluble in CO₂. Conversely, if the interaction energies between the surfactant and water are stronger, the surfactant may show better solubility in aqueous environments rather than in supercritical CO₂.

While Eq. (8) provides a useful framework, its application is limited by the accuracy of the input parameters (interaction energies), which are often derived from empirical or estimated data. Additionally, the equation assumes a simplistic interaction model that may not fully account for complex molecular interactions in heterogeneous reservoir environments. Therefore, future research should focus on refining the calculation of these interaction energies, potentially using more advanced techniques like quantum chemical calculations or molecular dynamics simulations, to improve the predictive accuracy of the model.

When supercritical CO₂ dissolves some solutes, the dissolution process can actually be regarded as the solvent-solute mixing process. The solubility parameters and volume fractions of solvents and solutes affect the mixing enthalpy during this process^[39], and the relationship is shown in Eq. (9).

$$\Delta H_m = V_m \varphi_1 \varphi_2 (\delta_1 - \delta_2)^2, \quad (9)$$

where ΔH_m represents the mixing enthalpy of the system; φ_1 represents the volume fraction of the solvent; φ_2 denotes the volume fraction of the solute; v_m represents the molar volume of the solution; δ_1 represents the solubility parameter of the solvent; and δ_2 represents the solubility parameter of the solute.

The change in Gibbs free energy in the dissolution process is shown in Eq. (10).

$$\Delta G_m = \Delta H_m - T \Delta S_m, \quad (10)$$

where ΔG_m represents the change in the Gibbs free energy of the system; ΔH_m represents the mixing enthalpy of the system; ΔS_m represents the mixing entropy of the system; and T represents the temperature of the system.

In general, the dissolution process tends to disrupt the molecular arrangement in the system, so $\Delta S_m > 0$. The dissolution process must satisfy $\Delta G_m < 0$, that is, $\Delta H_m - T \Delta S_m < 0$. Therefore, to achieve the condition of spontaneous dissolution, ΔH_m should be as minimal as possible. δ_1 and δ_2 should be as close as possible from Eq. (9), which is the principle of similar solubility parameters^[81].

The solubility parameter is currently an important measure of substance compatibility. To choose a reasonable and effective solvent, the solubility parameter is often used to evaluate the solvent. The traditional solubility parameters can be measured by experimental^[82] or theoretical estimation methods^[83]. However, the solubility parameters of a CO₂ supercritical fluid require a large number of targeted measurements under different conditions because they are susceptible to temperature and pressure. Some researchers have proposed some empirical equations, but these equations can only be qualitatively analyzed in most cases^[84]. Molecular dynamics simulation can also be used to investigate solubility parameters. Vimont et al.^[85] predicted the solubility parameters

of 51 common compounds by molecular dynamics simulation and quantum chemical semi-empirical molecular orbital, combined with multivariate minimum variance regression method. Xia et al.^[86] calculated the solubility parameters of 17 polar, nonpolar, and hydrogen-bonded organic solvents by the molecular dynamics method. The calculated results corroborated the experimental values.

Notably, the addition of alcohols as agents facilitates surfactant dissolution in supercritical CO₂ and promotes the formation of supercritical CO₂ microemulsions. Ethanol can adsorb at the oil–water interface. This phenomenon can reduce the interfacial tension, adjust the critical micelle concentration (CMC) and hydrophilic balance value, and increase microemulsion stability^[87,88]. Some theories suggest that alcohol molecules can permeate into the surfactant tail chain to reduce the interaction between surfactants^[89,90]. Zhang^[28] simulated the solubility parameters of a supercritical CO₂/alcohol agent system by molecular dynamics simulation, providing basic data for characterizing the influence of alcohol agents on supercritical CO₂ solubility. However, the role of alcohol agents in the surfactant system is still not sufficiently clear. The interaction mechanism between hydrocarbon surfactants/CO₂/agents needs to be continuously improved. Further research is also needed to develop a more convenient and accurate method for calculating the solubility parameters of supercritical CO₂.

2.3. Foam Generation and Stability

2.3.1. Foam Generation

Foam formation in porous media can be defined as the formation of a new foam lamella. Foam formation is a complex process, and its formation mechanism has basically reached a consensus, which can be divided into three cases: snap-off, lamellar division, and leave-behind^[91]. The first two cases produce strong foams, and the latter produces weak foams. These three mechanisms are the basis for understanding foam behavior in porous media, so they are introduced separately.

When Radke et al.^[92] first proposed the snap-off mechanism, they believed that snap-off was the most important mechanism for direct visual observation of foam formation. Kovscek et al.^[93] developed a fluid dynamics theory to describe the horizontal aggregation of liquid in narrow and angular pores under the action of a pressure gradient. They developed a statistical network model to describe the average rate of foam formation by detachment in porous media. As shown in Figure 8^[93], the foam will snap-off when the foam curvature difference between the front part of the foam and the contraction part is enough to cause the liquid flow to shrink back. Foam detachment can be divided into the following three cases: (1) When the upstream pressure exceeds the capillary pressure, the gas phase begins to invade the pore throat. The foam front enters the downstream pore, and the liquid phase rushes into the throat due to the capillary pressure gradient, after which the curvature of the foam front decreases with expansion. Rapidly flowing liquid phase forms a liquid ring until the foam snap-off. (2) When foams block the throat, the ensuing liquid pressure gradient drives the accumulated liquid upstream of the throat to clamp smaller foams. (3) The foam separates when the foam breaks away from a long straight channel. These three cases may occur in the absence of a surfactant. The static condition for snap-off is that the ratio of the pore throat to the channel is approximately 1:3, depending on the specific shape of the channel cross-section. This ensures that when the interface moves from the pore throat to the channel, the capillary pressure at the front of the interface is less than the capillary pressure at the throat^[65]. Some studies have shown that crude oil can affect foam snap-off. The snapped-off oil in the pores downstream of the pore throat will hinder or prevent the snapping-off of foams. This hinderance may be the result of insufficient surfactant concentration in the foam to prevent film rupture or an unstable oil phase surface of the pseudo-emulsified film.

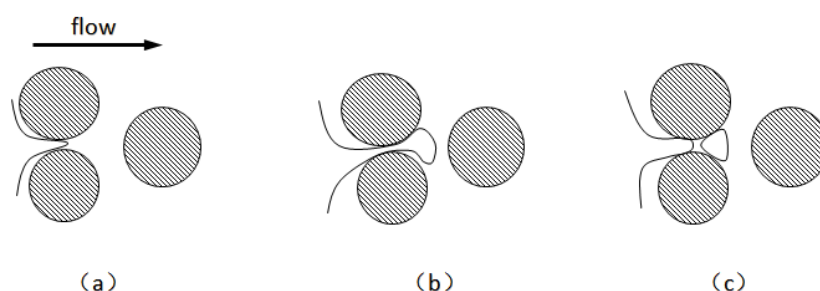


Figure 9. Foam snap-off process ((a) into pores (b) through pores (c) after passing through pores)
[93].

After the foams continue to build to create a large plate, they reach branching points during the migration process, which results in lamellar division because the large plate diffuses in two directions under the action of capillary force^[92]. The process of lamella division requires a large foam size, capillary force, and protruding rocks. Figure 9 shows the main mechanism^[93]. Chambers et al.^[94] also observed similar results in the foam flooding experiment of a micro-etching glass model. In porous media, lamella division occurs if the average size of foams is equivalent to or greater than the average size of pores. This means that lamella division occurs only when the lamella is present, so it is not the primary mechanism for foam formation. However, some studies have shown that lamella division is the main mechanism of foam generation^[93]. Furthermore, lamella division will not occur if the captured foam has occupied any of the channels. The new lamella is smaller than the original lamella when lamella division occurs. The frequency of lamella division is a function of the flow foam density, gas velocity, foam size, branching point, and capillary pressure^[52].

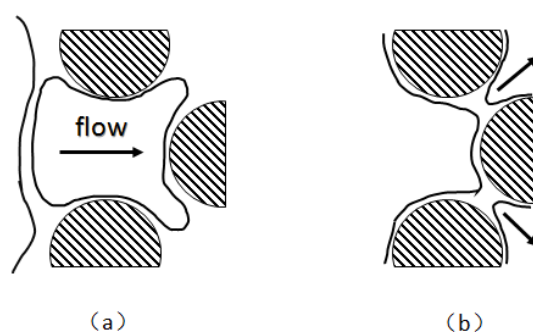


Figure 10. Lamella division diagram of foam ((a) before lamella division (b) after lamella division)
[93].

When the gas flows through an adjacent pore throat, the non-wetting phase replaces the wetting phase, and the two wet surfaces bridge together to form a lamella—the leave-behind occurs. A new lamella is formed at the pore throat between the two protrusions^[92]. As shown in Figure 10^[95], unlike the film perpendicular to the flow generated by snap-off and lamella division, the film is parallel to the flow that the leave-behind generates. The leave-behind generates a weak foam that cannot move initially. The effect of leave-behind is much lower than that of the snapping-off mechanism in terms of gas diversion capacity.

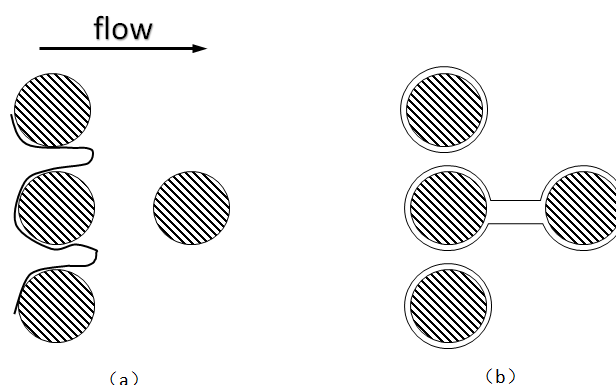


Figure 11. Schematic diagram of leave-behind ((a) before the foam through (b) after the foam through) [95].

2.3.2. Foam Stability

After the formation of new foams, the liquid film of the lamella will be thinner due to the disturbing force. The lamellae are unstable and tend to merge when the thinning process continues until the lamellae reach a critical thickness^[96]. While foam stability in porous media determines the oil displacement efficiency of foam, foam coalescence is the main factor affecting foam stability. Therefore, discussing the mechanism of foam coalescence is necessary.

Foams generally coalesce in porous media for the following two reasons: capillary-suction coalescence and gas diffusion^[94]. The capillary-suction coalescence is widely considered the main mechanism of film rupture. Liquid saturation, rock permeability, and surfactant concentration affect capillary force. Gas diffusion affects the capture of foams, and it is less common in porous media because the radius of the foam curvature is related to the pore throat and pore volume rather than the foam volume. The experiment shows that as the pore diameter of the porous medium is closer to the actual pore diameter of the reservoir, the foam duration is longer, indicating that "foam oil" will exist for a long time during the development of the reservoir.

The effects of varying film thicknesses on the lamella are also distinct. The thinning of relatively thick films (>100 nm) is primarily influenced by capillary force and gravity^[97]. In addition to gravity, the pressure gradient between the center and edge of the lamella primarily influences the thinning of horizontally thick films, as shown in Figure 11^[52].

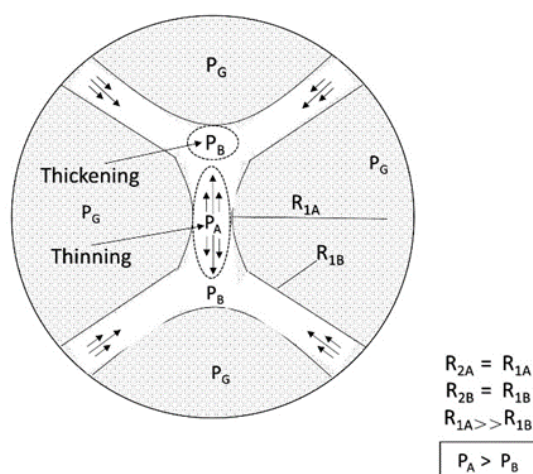


Figure 12. Pressure difference between the center and the edge of the lamella [52].

The thinning rate of the thick film is described in Eq. (11)^[60]. The formula shows that the film drainage rate is inversely proportional to liquid viscosity. Another factor that affects the stability of

thick film foams is the viscoelasticity of the foam surface—the Marangoni effect^[65]—which reduces the drainage rate of the films because it can prevent liquid flowing out from the high surface tension region of the film. The drainage time is proportional to the enhanced Marangoni effect^[98].

$$-\frac{dh}{dt} = \frac{2h^3 \Delta P}{3\eta R^2}, \quad (11)$$

where $-dh/dt$ represents the film thinning rate (m/s); h represents the instantaneous thickness of the film (m); ΔP represents the pressure difference between the center and edge of the sheet (Pa); η represents liquid viscosity ($Pa \cdot s$); and R represents the radius of foam (m).

The film drainage rate deviates from the calculation results of Eq. (11) when the thin film thickness is less than 100 nm mainly due to the enhanced separation pressure. Separation pressure retards film thinning through the interaction of long-range electrostatic repulsion (Π_{elec}), short-range steric hindrance (Π_{steric}), and short-range dispersion force (Π_{vdW}). The overlapping electric double layer around the two lamella interfaces produces $\Pi_{electro}$ ^[52]. Its strength depends on the electrolyte concentration in the aqueous phase and the charge density at the gas–liquid interface. The hindrance to the film thinning interaction between the lamella interfaces and film structures produces Π_{steric} . The structures that provide resistance may be entangled polymers, layered oil droplets, layered spherical micelles^[52], or entangled columnar micelles^[99]. Π_{vdW} is usually an instantaneous induced dipole attraction between two particles located at the lamella interface. Its strength depends on the material density of the adjacent phase. However, the separation pressure is mainly aimed at the behavior of static lamellae, and it cannot describe the dynamic behavior. Khatib et al.^[46] found that a flowing foam has a limit capillary pressure (P_c^*), which means that a critical water saturation (S_w^*) exists. As shown in Figure 12^[66], lower water saturation leads to higher capillary pressure. When P_c exceeds P_c^* , the foam becomes unstable. The stability of a flowing lamella determines the stability of a flowing foam without oil. When the lamella becomes thin to a critical thickness, it breaks.

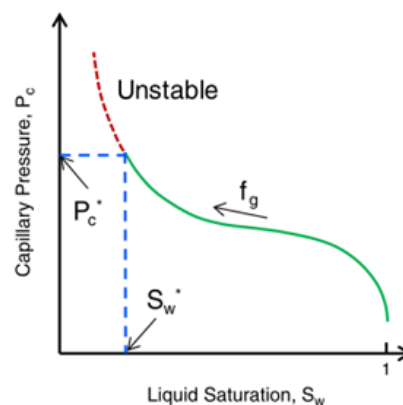


Figure 13. Capillary pressure curve (f_g is gas fraction flow) ^[66].

It may inhibit foam formation and reduce foam stability when the foam contacts different phases (including the oil phase). The influence of the oil phase on foam stability depends on the structure of the oil, surfactant, and water phases^[100], which can be expressed by three interaction parameters: diffusion, entry, and bridging coefficient.

Diffusion coefficient (S): If the affinity of the oil to the new phase is strong, the oil diffuses at the gas–liquid interface to form a film when the oil contacts the gas–liquid interface, but if the affinity of the oil to the new phase is weak, the oil will form small droplets at the interface. The diffusion coefficient is a function of the interfacial tension of oil, gas, and surfactant relative to each other, as shown in Eq. (12). If the expansion coefficient S is positive, the oil diffuses on the foam. This often leads to foam instability.

$$S = \gamma_{S/G} - \gamma_{S/O} - \gamma_{O/G} \quad (12)$$

Entry coefficient (E): An insoluble reagent may enter the gas–liquid interface when the insoluble reagent (such as oil) disperses inside the foam film. A new gas–oil interface will be generated if the entry coefficient is positive after the oil has entered the gas–liquid interface and some oil–surfactant and gas–surfactant interfaces are destroyed, resulting in interfacial film instability. Oil dispersion in the film does not necessarily lead to foam instability^[61]. Theoretically, if the entry coefficient is negative, the oil will flow out of the film surface and will not render the foam unstable. When the number of films is small, the foam is the most stable^[100].

$$E = \gamma_{S/G} + \gamma_{S/O} - \gamma_{O/G} \quad (13)$$

Bridging coefficient (B): The oil may bridge adjacent foams if the oil enters the gas–liquid interface but does not diffuse. When the bridging coefficient is positive, the film is unstable, whereas when it is negative, the film is stable. The equation is as follows:

$$B = (\gamma_{S/G})^2 + (\gamma_{S/O})^2 + (\gamma_{O/G})^2 \quad (14)$$

In addition, factors such as temperature, surfactant concentration, salinity, and solid particles affect foam stability.

In general, foam stability decreases with increasing temperatures. The drainage time decreases and foam rupture speed increases when temperature increases^[98,101,102]. Below the CMC, the increase in concentration results in a decrease in interfacial tension and stabilization of the foam. Nikolov et al.^[103] realized improved foam stability when the surfactant concentration markedly exceeded the CMC. Depending on the type, concentration, salinity, and divalent ions of surfactants, salinity may enhance or suppress foam stability. The effect of pH on foam stability is relatively small when the concentration is above the CMC^[32].

Solid particles may enhance or decrease foam stability. If the particles are not hydrophilic, their aggregation at the foam interface can enhance the film mechanical stability and can also increase the stability by increasing the overall viscosity when dispersed^[61]. Nanoparticle-stabilized foams have shown promising results in improving foam stability, especially under harsh reservoir conditions. Studies have demonstrated their ability to maintain foam integrity over extended periods, even in unconventional oil recovery scenarios^[70–72]. Nanoparticles play a role in foam stability mainly by increasing the mechanical strength of the lamella, increasing the maximum capillary pressure, and forming a network structure^[104]. The adsorption of nanoparticles on the lamellae is one of the main mechanisms of foam stabilization by nanoparticles. Compared with surfactants and polymers, nanoparticles have higher separation energy and specific surface energy due to their small size^[105]. Therefore, nanoparticle adsorption on the gas–liquid film is irreversible^[106] and can prevent gas diffusion and foam coalescence. Nanoparticles with moderate hydrophobicity tend to adsorb on the gas–liquid interface and are more stable in the membrane^[107]. Therefore, moderately hydrophobic nanoparticles have better foam stability than extremely hydrophobic or extremely hydrophilic nanoparticles. In addition, the interaction between nanoparticles is another important mechanism affecting foam stability. There may be three structures—single layer, thick multilayer, and network structure—when nanoparticles are dispersed in a foam solution^[108–110]. While the network structure promotes the stability of maximum capillary pressure and separation energy and enhances the energy demand of foam coalescence^[111], it prevents the film from thinning, reduces gas diffusion and liquid discharge, thereby preventing small foams from merging into large foams and prolonging the existence time of the foam system^[112,113].

During the channeling process, when carrying surfactants, the CO₂ phase interacts with the water phase in the pore to generate foam. Therefore, the crossflow of CO₂ favors the acceleration of foam generation in the core with high permeability, making the foam plugging effect faster. The surfactant carried in the CO₂ phase facilitates foam regeneration after the foam ruptures during foam migration, thereby prolonging the foam stability time^[28].

2.4. Flow and Rheological Model of Foam

CO₂ foam with good stability is required in the application process. Recent studies have advanced the understanding of foam stability through visualization techniques, showing real-time foam behavior and enhancing predictions of foam stability^[114,115]. Compared with the unsteady foam

flow study based on relative permeability and viscosity, the steady foam study prioritizes foam fluidity^[54]. The sole function of liquid saturation that influences foam fluidity is foam size and structure^[116,117]. These two parameters are affected by many factors, such as foam properties, gas content in foam, pore structure, medium heterogeneity, surfactant system, capillary pressure, flow rate, and non-wetting^[52,54].

When the pore size of a porous medium exceeds the diameter of a single foam, the foam is referred to as bulk foam^[118], and multiple foams then accumulate in the pore space. As shown in Figure 13a^[97], while the bulk foam features easily separable spherical foams when the gas content is low, it features polyhedral foam (also known as dry foam) when the gas content is high. However, the average foam size is usually larger than the pore size; that is, a single foam occupies more than one pore space^[66]. Foam in porous media typically comprises continuous and discontinuous foams. Discontinuous foam is divided into flowing and retention foams. As shown in Figure 13b^[119], the discontinuous foams occupy large and medium pores. Flowing foam usually occupies the largest pores, whereas retention foam occupies small and medium pores. Foam mobility depends on the gas pressure gradient and foam size. Flowing foam and retention foam are dynamic.

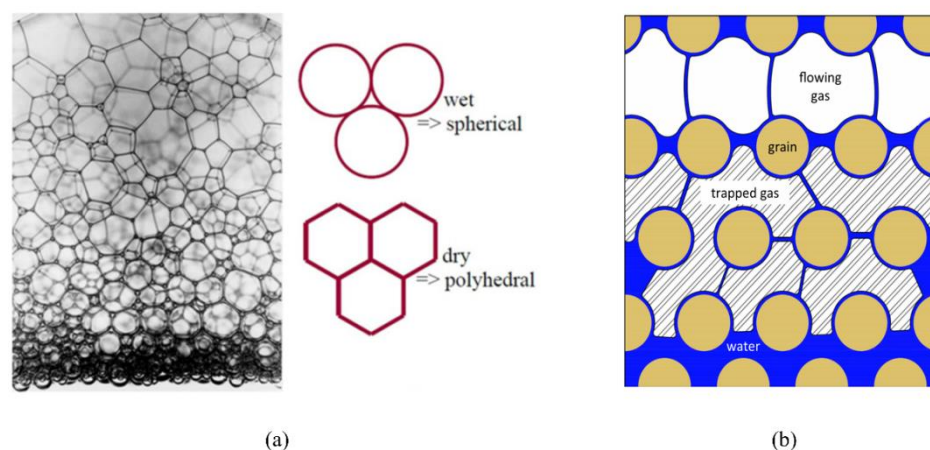


Figure 14. Forms of foam existence ((a) bulk foam ^[97] (b) foam in porous media ^[119]).

Foam reduces liquidity by reducing effective gas permeability and increasing gas flow resistance. Both flowing and retention foams can cause flow resistance. The lamellae reduce the effective permeability of the gas flowing through the connected channels by the required pressure of the shrink pore throat. The effective yield stress of the lamella to the gas will also capture a considerable part of the gas under a high pressure gradient, thereby hindering gas flow^[52,59,120]. The retention foams block the pores to reduce the channels available for gas flow and lower the effective permeability of gas. The foam structure dominates foam rheology, and the porous media regulates the foam structure through capillary pressure when the foam flows in the porous media. The viscous shear stress of the film between the hole wall and the lamellae increases the apparent viscosity, as shown in Figure 14^[121]. When the foam flows, the wetting film covering the pore wall interacts with the lamella. The conditions of equilibrium between the two films are the primary determinants of foam equilibrium. The thermodynamic properties of the two films may dominate foam behavior. This effect is particularly pronounced in strong foams, where the wetting film and lamella limit all foams. Because viscosity and capillary force affect foam flow at any time, foams in the mobile phase will exhibit an obvious dragging phenomenon when passing through the contraction pore throat, resulting in an irregular lamella movement. When the lamellae reach the contraction portion of the channel, their movement accelerates, and their centers become convex backward. However, when the lamellae separate from the pore throat, their movement slows, and their centers become convex forward. When there is constant pressure, the lamellae do not generally move steadily but move alternately by sliding and stopping. This movement is known as the stick-slip motion^[122].

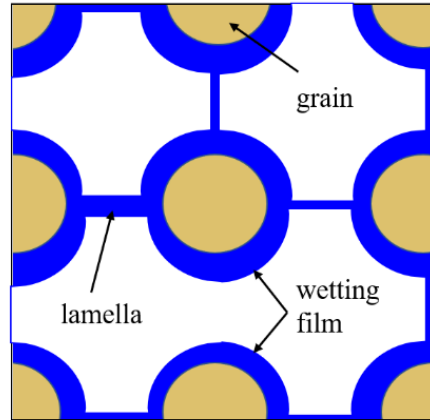


Figure 15. Gas and liquid distribution diagram of strong foam in porous media ^[121].

Numerous researchers have examined the simulation of foam behavior. Because the factors influencing foam fluidity are numerous and complicated, it is difficult to precisely forecast foam behavior. However, some researchers have proposed many methods to simulate foam flow in porous media. Most models change gas fluidity when foam is generated. These foam models can be roughly divided into four categories^[123], empirical or semi-empirical models (empirical changes in gas mobility), theoretical models of separated-phase flow (including critical capillary force model^[124], pore network model^[125], foam overlay and drainage model^[126], and foam structure evolution model^[127]), seepage (statistical network) model,^[128] and mechanical model (population balance model)^[129]. The following introduction focuses on empirical or semi-empirical modeling and mechanical modeling methods.

2.4.1. Empirical or Semi-Empirical Models

Because the empirical or semi-empirical model is not a function of the foam structure and gas fluidity but a function of the steady-state gas flow, it is necessary to empirically correct the relative permeability and viscosity of the gas separately or simultaneously. To characterize the function of liquidity reduction, researchers have incorporated the micro-foam process into empirical or semi-empirical models. As a result, no additional conditions are required for the continuity equation or the rate equation of all phases. Two popular empirical models are as follows:

(1) STARSTM foam model

STARSTM is a commercial foam model developed by the Computer Modeling Group in Calgary, Canada^[130]. The basic assumption is that foam formation and coalescence occur rapidly compared with the flow, so the foam exists whenever the gas and surfactant aqueous solution coexist. The concept of liquidity reduction factor is proposed as a weighting factor to determine the relative permeability of gas to different foam strengths. The equation is as follows:

$$k_{rg}^f = k_{rg}^o S_w * FM \quad (15)$$

The dimensionless interpolation factor FM is in the range of 0–1, where 0 represents a very strong foam and 1 represents no foam. The influencing factors of the value are as follows:

$$FM = \frac{1}{1 + fmmob * F1 * F2 * F3 * F4 * F5 * F6 * F7} \quad (16)$$

In the formula, FM represents the liquidity reduction factor varying between FM = 1 (no foam) and FM < 1 (strong foam). fmmob represents the reference foam fluidity reduction factor. f₁ represents the effect of surfactant concentration. f₂ represents oil resistance. f₃ represents the influence of the capillary number. f₄ represents the effect of capillary number on foam formation. f₅ represents the oil component impact. f₆ represents the salinity effect. f₇ represents the dry out effect.

(2) UTCOMP foam model

The UTCOMP model is a foam miscible flooding model. Liu^[131] and Chang et al.^[132] proposed the UTCOMP model modified based on the “fixed- P_c^* ” model. The “fixed- P_c^* ” model is a stable state in which layers are maintained in a local equilibrium between foam formation and coalescence when the capillary force dominates the foam structure and gas flow. It describes the local equilibrium state of strong foam. The basic assumption is that the foam structure only adjusts the fluidity of the foam itself and the gas according to demand. Thus, the water saturation stabilizes at S_w^* , ensuring that the critical capillary pressure (P_c^*) is independent of the gas–liquid flow rate^[133,134]. Therefore, the model does not describe the slow formation or coalescence of foams, nor does it describe a flow rate-dependent process. In general, P_c^* is affected by factors such as rock properties, surfactant formulation, concentration of each component, and temperature. In some cases, flow rate and foam quality also affect P_c^* ^[46]. The surfactant concentration and oil saturation can form a smooth function curve that affects foam strength based on the continuous behavior of foam at the surfactant concentration of C_s^* ^[135]. S_w^* increases with increasing flow rate, and P_c^* increases with decreasing permeability^[46,133]. UTCOMP only represents the effect of foam by changing the relative permeability (k_{rg}) of the gas for easy application.

In the early UTCOMP foam model^[136], there are two additional conditions, $S_g > S_{g,lim}$ and $S_o < S_{o,lim}$. In the current UTCOMP model, if the surfactant exists, its concentration surpasses a specific value (C_s^*), and the water saturation also exceeds a specific threshold (S_w^*), the foam will then be formed. Make the following changes to k_{rg}^f in the model:

If $S_w \leq S_w^* - \varepsilon$ or $C_s < C_s^*$, then

$$k_{rg}^f = k_{rg} \quad (17)$$

If $S_w^* - \varepsilon \leq S_w \leq S_w^* + \varepsilon$ and $C_s \geq C_s^*$, then

$$k_{rg}^f = \frac{k_{rg}}{1 + \frac{(R-1)(S_w - S_w^* + \varepsilon)}{2\varepsilon}} \quad (18)$$

If $S_w > S_w^* + \varepsilon$ and $C_s \geq C_s^*$, then

$$k_{rg}^f = \frac{k_{rg}}{R} \quad (19)$$

The foam exhibits shear-thinning behavior in the low-mass region after the gas flow rate is modified by the foam parameter (R).

$$R = R_{ref} \left(\frac{u_g}{u_{g,ref}} \right)^{\delta-1} \quad (20)$$

Shi^[137] introduced two other new parameters into the model to study the change trend in foam fluidity in low-quality areas on this basis. Jose^[138] comprehensively analyzed the research situation of high-quality area and low-quality area^[139] models and then proposed a unified “ f_g^* model” for the two areas.

The foam model in the fluid-flowing models of STARSTM and UTCOMP can also be called a heuristic model or local population balance model because they are the methods between experience and population balance. This model keeps the simplification of the former and avoids the complex calculation of the latter. However, due to the use of case-specific methods, empirical models generally lack versatility.

2.4.2. Population Balance Model

Calculating mass and energy transfer in porous media enables researchers to add foam to reservoir simulation using the population balance method—a mechanical method developed based on the concept of tracking the number of foams. This method can quantify the relationship between foam fluidity and structure while separating and defining the formation and rupture mechanism of liquid film or lamella of foams^[52,59,140]. The population balance model, which can be subdivided into the population balance model and the local population balance model, is the theoretically most comprehensive foam model framework. The population balance model is a method of tracking the

change in the foam structure (n_f) based on mass conservation^[129]. The n_f sometimes is referred to as the lamella density of the flowing foam in order to distinguish it from the foam structure (n_t) of the trapped foam^[95].

However, a significant number of parameters of laboratory research and field data are difficult to precisely integrate into the model, limiting the population balance method's use in practice. The cost of directly solving the population balance equation is too high, and a divergence problem exists. Therefore, some scholars have proposed a method to obtain foam density by the number of foams or local balance. This method assumes that foam formation and coalescence are relatively fast compared to the time scale of foams passing through the porous media, and the dynamic equilibrium of the local foam structure is achieved by equalizing the local foam formation (R_g) and coalescence (R_c) rates^[45,141,142]. The model is multiphase and multicomponent, which can represent mass transfer between phases and foam dynamics. In addition, the model can predict a wider behavior of the foam dispersion process under different experimental conditions.

The general form of the population balance model is Eq. (21)^[143]. From left to right is the cumulative term of flowing and trapped foams, the flow rate of flowing foams, the source term of the net generation term and the foam. S_g and S_{gt} are related to S_{gf} (Eq. (22)). In the equation, X_t is the flow gas fraction, and X_t is the retention gas fraction. The relationship between X_t and the maximum retention gas fraction $X_{t,max}$ is shown in Eq. (23); β is the retention parameter.

$$\frac{\partial}{\partial t}(\phi(S_{gf}n_f + S_{gt}n_t)) + \nabla \cdot (u_g n_f) = \phi S_g(R_g - R_c) + Q_b \quad (21)$$

$$S_{gf} = X_f S_g = (1 - X_t) S_g, S_{gt} = X_t S_g \quad (22)$$

$$X_t = X_{t,max} \left(\frac{\beta n_t}{1 + \beta n_t} \right) \quad (23)$$

Bertin et al.^[142,144,145] proposed a relation that expresses the change in flow foam density with the physical properties of porous media (porosity, permeability, and capillary pressure), surfactant solution, and flow conditions based on many assumptions. The relation expression is feasible at both pore and core scales. The grain diameter can estimate the amount of porosity per unit volume and can be evaluated simply by the Kozeny–Carman relation. Li et al.^[146] established foam models to simulate one-dimensional and three-dimensional foam flow. They did not directly correct the gas relative permeability but proposed an alternative method that considers the interception of gas to simply increase the gas residual saturation when calculating the gas relative permeability. The model calculates the gas apparent viscosity through the formula of Friedmann et al.^[59] that considers the shear-thinning effect and uses the formula of Bertin et al.^[145] to express the foam density (foam structure). Five regions of gas saturation increase are defined and discussed based on this, and the expressions of gas apparent viscosity differ. Chen et al.^[147] extended the computing power of previous models to low-quality areas by considering the dependence of foam formation on the existing foams when calculating the foam formation rate, because of the limitations of the existing population balance model. They also proposed and implemented a new simplified foam model for the efficient simulation of foam displacement in porous media using the simplified expression of foam generation and the local equilibrium assumption of foam generation and coalescence.

The population balance model obtains the foam structure by solving the partial differential equation based on the general form. The local population balance model obtains the foam structure by solving the algebraic equation of variables obtained by Darcy's law and mass conservation equation based on the semi-empirical or population balance model. All the above quantitative equilibrium models solve only two problems: how to obtain n_f (the function of gas saturation, trapped gas fraction, and capillary pressure) and how to change foam fluidity. Due to the different methods of describing slice generation, the expressions of these models also differ. In other words, both the population balance and local population balance models are set to correct only the relative permeability (k_{rg}) or apparent viscosity (μ_g) in porous media. Most quantitative equilibrium models change the gas relative permeability by multiplying with the flow gas saturation, and change the gas

apparent viscosity by η_{app} in the capillary. Applying a suitable formula to describe the phenomenon of trapped gas is key to adjusting the relative permeability of gas (k_{rg}).

Thus far, no single foam model can be applied to all foam experiments in porous media under different conditions using foam mobility modeling technologies. Therefore, fitting laboratory or field data to modeling parameters is particularly important for establishing and validating foam models. Due to the variances across the models, their fitting methods differ. Therefore, establishing appropriate assumptions based on actual data during foam flooding is necessary, as is considering the impact of crude oil on foam stability, liquidity, and other major control factors in the foam flow mechanism.

2.5. CO₂ Foam EOR Mechanism

Foam formation and coalescence affect gas flow during CO₂ foam flooding. A rheological model can describe the flow characteristics of foam in porous media and can be used to analyze the effect of foam on gas fluidity. However, the CO₂ foam displacement effect is multifaceted, and its specific mechanism in the experimental process needs to be discussed. CO₂ foam can effectively reduce CO₂ fluidity and stabilize the displacement front while significantly improving the crossflow and gravity separation caused by pure CO₂ injection. The decrease in gas flow is due to the increase in apparent viscosity and trapped gas fraction^[54]. Zhang et al.^[87] found that AOT dissolution in supercritical CO₂ can increase supercritical CO₂ viscosity by three times, and the formation of supercritical CO₂ foam can increase viscosity by 50–200 times. Foam can produce effective yield stress on gas^[115]. Even under a high pressure gradient, CO₂ foam can capture a considerable part of gas and hinder gas flow. The static or trapped foam can lower the effective permeability of gas by reducing some porous media available for gas flow, thereby blocking the gas flow channel^[59,120]. No maximal pressure gradient may mobilize all foam lamellae during core displacement. This means that the porous media always bound some foams during foam flow^[123]. The proportion of foam-bound gas in sandstone is about 85%–99% under steady-state conditions. Foam mobility and gas–liquid interface rearrangement affect gas flow. The additional pressure drop driving the foam at a constant speed exceeds the same volume of liquid, indicating that foam can increase the effective viscosity of the gas phase^[148]. The surfactant movement at the gas–liquid interface produces a surface tension gradient, which slows down the foam movement and increases the effective viscosity of the foam^[61].

Foam can selectively block heterogeneous media and improve CO₂ sweep efficiency. As shown in Figure 15^[149], the foam reduces the relative permeability of the gas by blocking the pores of the gas flow and transferring the flow from the area with higher permeability to the untouched area with lower permeability. Foam or gas plugging occurs at the boundary under sufficient permeability differences^[150]. The influence of limit capillary pressure on foam lamella is often used to explain the relationship between pressure gradient and gas–liquid flow rate in high-quality area^[46]. The limit capillary pressure is also affected by permeability^[141]. Foam diversion is sensitive to permeability in high-quality areas and insensitive to permeability in low-quality areas, but the effect of channeling in low-quality areas improves significantly. This permeability dependence makes foam particularly suitable for improving interlayer heterogeneity^[151]. Notably, the competition between gravity (and density difference) and transverse pressure gradient^[152] leads to gravity superposition. As the displacement front advances away from the injection well, the pressure gradient and velocity decrease, increasing gravity overpressure. This effect is the same in the cylindrical flow with a fixed injection velocity^[137]. Foam can effectively overcome the influence of gravity and improve the CO₂ sweep efficiency.

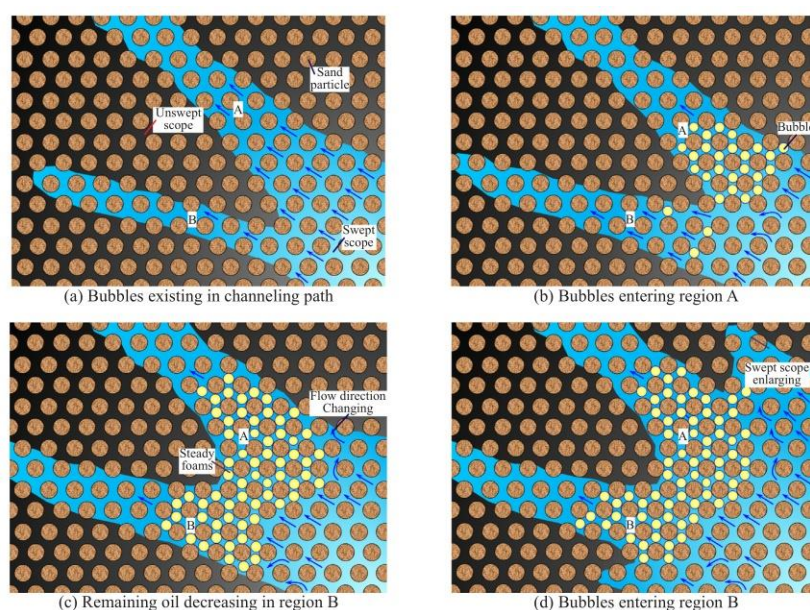


Figure 16. Increased sweep range by foam plugging ((a) bubbles existing in channeling path (b) bubbles entering region A (c) remaining oil decreasing in region B (d) bubbles entering region B) ^[149].

Surfactant addition can reduce capillary force and alter rock surface wettability by reducing the oil–water surface IFT. It is beneficial to separate oil from porous media. The oil can form emulsions under reservoir conditions and is easy to displace. As shown in Figure 16^[153]. The oil–rock adhesion far exceeds the capillary force that keeps oil on the rock surface in the oil-wet reservoirs. The ability of surfactants to change wettability (rather than reduce IFT) and the diffusion behavior of oil in three fluid (oil, brine, and gas) systems dominate oil displacement^[155].

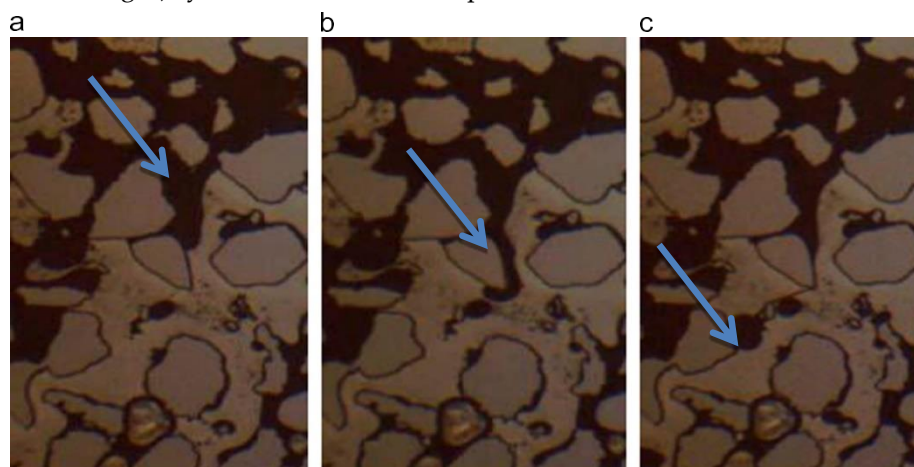


Figure 17. Changes in rock wettability facilitate the displacement of residual oil ((a) After water flooding, the residual oil is prevented from passing through pores by capillary forces (b) The residual oil is mobilized when it comes into contact with an alkaline surfactant (c) The mobilized oil mass is pulled into the flow channel to form a microscopic oil droplet that is eventually washed away by water flow) ^[153].

In porous media, retention foam can persist for a long time. There is a long-term contact of CO₂-film-oil three phases when it is in contact with undisplaced oil. The interfacial mass transfer between CO₂ and oil is strengthened. This makes the mass transfer of CO₂ to the oil increase and enhances the viscosity reduction and expansion of oil^[148,156]. Because high pressure can significantly enhance the mass transfer of CO₂ into water and oil (n-decane) when a surfactant exists^[157], measuring the effect of surfactants on the degree of mass transfer at higher pressures is necessary^[158]. Oil will also migrate

to the lamella structure of the foam via emulsification dialysis, pseudo-emulsification film thinning, entry, and diffusion. The oil will be emulsified into the aqueous phase, resulting in oil and gas separation of aqueous film as long as the foam diffuses in the crude oil—the pseudo-emulsified film. Notably, if the oil diffuses on the foam, it will diffuse on or penetrate the lamella surface and destroy the lamella inner surface^[61]. More crude oil will destroy the foam^[159], and CO₂ will make direct contact with the crude oil.

3. Classification and Application Progress of CO₂-Soluble Surfactants

In this section, we classify the common surfactants in the petroleum industry and describe the screening criteria and parameters of CO₂-soluble surfactants, after which we introduce the application progress of each type of surfactant (ionic and nonionic surfactants and mixed surfactants) in CO₂ foam flooding.

3.1. Surfactant Classification

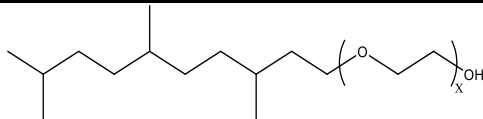
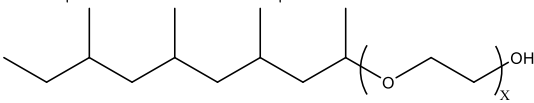
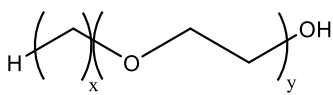
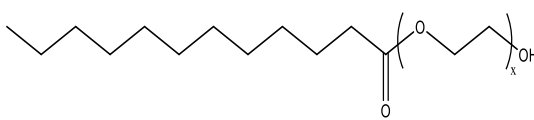
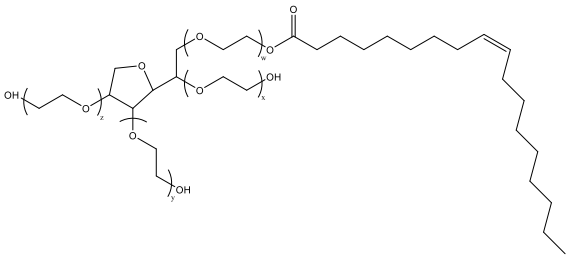
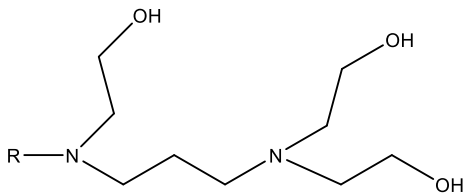
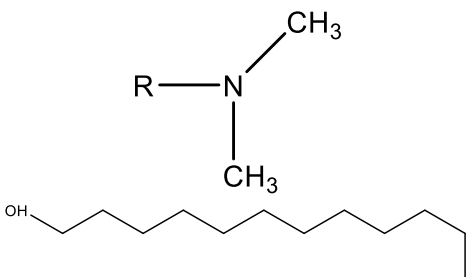
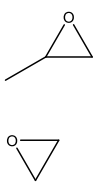
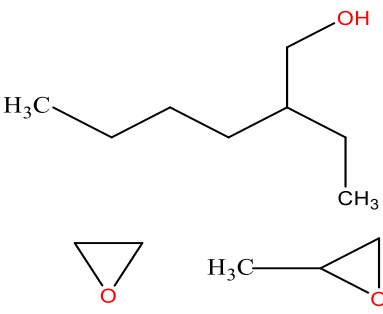
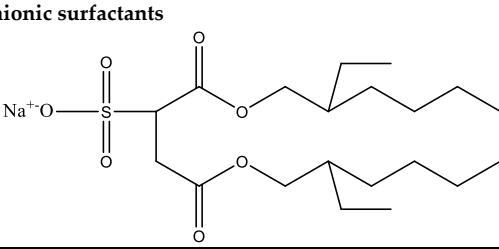
Surfactants typically comprise hydrophilic head and hydrophobic tail groups. According to the polarity of the head group, they are divided into nonionic and ionic surfactants. The ionic surfactants can be subdivided into cationic, anionic, and zwitterionic surfactants^[160].

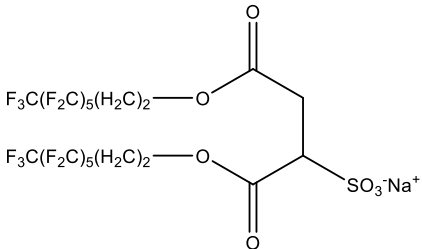
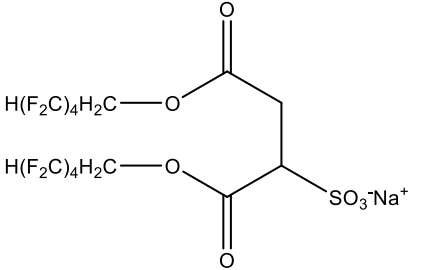
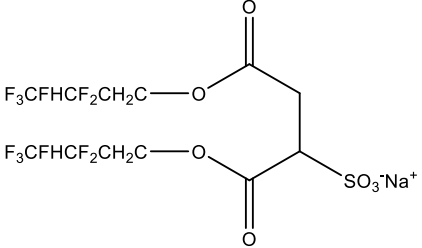
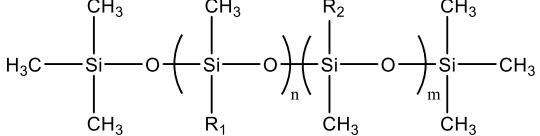
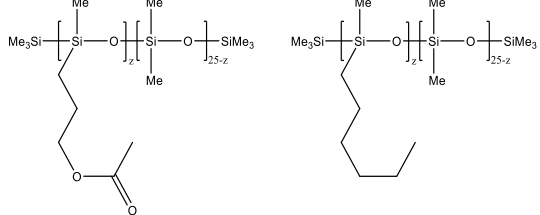
Nonionic surfactants have no charge on the head group. Non ionic surfactants typically have high solubility in organic solvents, making them suitable for use in various solvent systems and exhibiting good stability. The common CO₂ soluble nonionic surfactants are mostly ethoxylates and amine derivatives. Ethoxylates can be divided into branched alkylphenol ethoxylates, branched alkyl ethoxylates (branched ethoxylate alcohols), nonbranched alkyl ethoxylates (linear ethoxylate alcohols) and fatty acid-based surfactants. Among them, the common branched alkylphenol ethoxylates include 2-(2-[4-(1,1,3,3-tetramethylbutyl)phenoxy]ethoxy)ethanol, nonylphenol branched ethoxylated, and tristerylphenol ethoxylated. Common branched alkyl ethoxylates include polyethylene glycol trimethylnonyl ether, ethoxylated isodecyl alcohol, C₁₂–C₁₄ fatty alcohols ethoxylated, and GENAPOL(R) X-080. The common nonbranched alkyl ethoxylates include alkyl-(C₁₀–C₁₄) alcohol, ethoxylated. Common fatty acid-based surfactants include polyethylene glycol monolaurate and polyoxyethylene 20 sorbitan monooleate^[25,161]. Amine derivatives mainly include N, N', N' - polyoxyethylene(10)–N–tallow-1,3-diaminopropane (DTM), N-oleyl propylene diamine polyoxyethylene ether, coco alkyl dimethylamines, and ethoxylated cocoamines, among which ethoxylated cocoamines also belong to nonbranched alkyl ethoxylates^[162,163]. In addition, there are some other nonionic surfactants, including propoxylated and ethoxylated dodecanol, oxirane, methyl-, polymer with oxirane, mono(2-ethylhexyl) ether, and modified alkylphenol polyoxyethylene ether. Among them, when DTM and ethoxylated cocoamines are dissolved in an acidic aqueous solution (the pH of an aqueous solution containing CO₂ is generally 4–5), due to the protonation of the amine head group, the surfactant will change from nonionic to cationic, which has great application potential. The above nonionic surfactants have good solubility under high temperature, high pressure, and high salt, and their adsorption capacity in carbonate reservoirs is very low^[101]. The specific information is shown in Table 3, where N–X is a representative alkyl tail, and the actual surfactant comprises mixed isomers, which is a qualitative characterization in the table.

The ion surfactant has good foaming performance and foam stability. However, due to structural characteristics, the solubility of most ion surfactants in CO₂ is extremely limited, which limits their application. At present, there are few soluble ionic surfactants for CO₂, and the common anionic surfactants are AOT and sodium dodecyl sulfate (SDS)^[31,87]. Research on cationic surfactants mainly focuses on convertible ethoxylated amine surfactants, such as N,N',N'-trimethyl-N-(tallowalkyl)-1,3-propanediamine (DTM) and ethoxylated cocoamines^[164]. Common zwitterionic surfactants are mainly betaines, such as cocoyl amide propyldimethyl glycine (CAB-35)^[31] and lauroylamide propylbetaine^[165], and N-dodecyl-N,N-dimethyl-3-ammonio-1-propanesulfonate^[23].

Table 3. Summary of common CO₂-soluble surfactants.

Surfactants	Trade name	Chemical expression	CAS
Nonionic surfactants			
2-(2-[4-(1,1,3,3-Tetramethylbutyl)phenoxy]ethoxy)ethanol	Dow Triton X 100 (x=10), BASF Lutensol OP 10 (x=10), Huntsman SURFONIC® OP-100 (x=10), OP-120 (x=12)		9036-19-5
Nonylphenol branched ethoxylated	Huntsman SURFONIC® N-120, N-150, N-200, N-300, N-400, x=12, 15, 20, 30, 40.		127087-87-0
	Dow Tergitol NP9,12,15 (x=9, 12, 15)		127087-87-0
	Stepan Cedepal CO 630, 710, x=10 and 10.5		127087-87-0
Tristyryl phenol ethoxylated	Huntsman XOF-501		99734-09-5
Polyethylene glycol trimethylnonyl ether	Dow trimethylnonyl Tergitol TMN 6		60828-78-6
Ethoxylated isodecyl alcohol	BASF Lutensol XP 70		61827-42-7

C ₁₂ -C ₁₄ fatty alcohols ethoxylated	BASF Lutensol TO 8, 10		68439-50-9
GENAPOL(R) X-080	Huntsman SURFONIC® TDA-8, 9		9043-30-5
Alkyl-(C ₁₀ -C ₁₄) alcohol, ethoxylated	Huntsman SURFONIC® L12-8; BASF Lutensol AO8, AO11		66455-15-0
Polyethylene glycol monolaurate	Sigma Aldrich PEG monolaurate 600		9004-81-3
polyoxyethylene 20 sorbitan monooleate	Tween 80		9005-65-6
N,N',N'-polyoxyethylene (10)-N-tallow-1,3-diaminopropane	Ethoduomeen T/13		61790-85-0
Coco alkyldimethylamines	Armeen DMCD		61788-93-0
Propoxylated and ethoxylated dodecanol	-		68238-81-3
Oxirane, methyl-, polymer with oxirane, mono(2-ethylhexyl) ether	-		64366-70-7
Anionic surfactants			
Diocetyl sulfosuccinate sodium salt	AOT		577-11-7

			di-HCF7
Fluorine-containing AOT homologue	-		di-HCF4
			di-HCF3
Oligosiloxane	-		-
Functional silicone	-		-

In addition to the surfactants listed above, there are several more. In the early stages of CO₂ gas-soluble surfactant research, fluorine- and silicone-containing surfactants were proposed. They include perfluoropolyether ammonium carbonate, double-tailed fluorocarbon sulfate, double-tailed fluorocarbon-hydrocarbon mixed sulfate, fluorine-containing dialkyl phosphate, fluorine-containing AOT homolog, oligosiloxane, and functional silicone^[28]. Because these surfactants have small cohesive energies, good molecular chain flexibility, low glass transition temperatures, and small intermolecular interactions^[166], they can readily dissolve in CO₂^[167,169]. Fluorine- and silicon-containing surfactants readily solubilize in CO₂ and exhibit excellent foaming properties and foam stability. Although they are very good CO₂-soluble surfactants, cost inefficiency and environmental toxicity^[169] greatly limits their application.

In addition to using a single surfactant, researchers have mixed cationic, anionic, and nonionic surfactants separately. Because the synergistic effect of different types of surfactants can improve gas fluidity, various surfactant blending systems have been developed, including different ionic surfactant blending systems such as anionic sodium dihexyl sulfosuccinate + cationic benzethonium chloride^[170], anionic F-OPT + cationic F-CAT^[169], bis(1H,1H,2H,2H - heptadecafluorodecyl) -2-sulfosuccinate and fluorocarbon-hydrocarbon hybrid anionic surfactants^[172], as well as nonionic surfactant blending systems such as C₁₂NEO₂ + C₁₃EO₁₂^[173]. Table 4 lists their specific descriptions.

Table 4. CO₂ soluble surfactant blend systems.

Surfactant	Remarks	Reference
Double-tailed anion: sodium dihexyl sulfosuccinate (SDHS). Unbalanced-tail (different tail lengths) cation: benzethonium chloride (BCl)	Microemulsions can be formed without adding alcohol. Compared with the use of anionic surfactants alone, the mixture exhibited a higher critical microemulsion concentration. Under the optimal microemulsion conditions, the mixed anionic-cationic surfactant system solubilizes more oil than the anionic surfactant alone.	[170]
Anionic: F-OPT. Cationic: F-CAT	At high temperature (80°C), high salinity (160g/L TDS), high hardness (R+=0.3), pressure (120bar) conditions can be effectively dissolved. The mixed system can reduce the adsorption of carbonate powder. Under supercritical CO ₂ (40°C/120bar) conditions, the half-life of volume foam in carbonate minerals (99% alcite) achieves a low static state of 24h.	[171]
Anion: Sodium bis(1H,1H,2H,2H - heptadecafluorodecyl)-2-sulfosuccinate (8FS(EO) ₂); fluorocarbon–hydrocarbon hybrid anionic surfactants (FC6-HCn)	In the presence of excess water, the mixed surfactant can prevent the conversion of the microemulsion to the liquid crystal phase. At the same time, it was found that the micro-separation of 8FS(EO) ₂ and FC6-HCn formed a loose molecular accumulation, which enhanced the stability of the mixed microemulsion and the area occupied by each surfactant molecule.	[172]
2 ethoxylated amine headgroups with cocoalkyl tails (C ₁₂ NEO ₂) and nonionic surfactant with high degree ethoxylation (C ₁₃ EO ₁₂)	There is a positive synergy between the two surfactants, which can effectively improve the foam stability. When the C ₁₃ EO ₁₂ ratio is less than 30%, the cloud point pressure increment will be less than 20%. At the optimum ratio, the apparent viscosity of foam increases by about 2.5 times.	[173]

3.2. Application Progress

3.2.1. Nonionic Surfactants

Due to their relatively good solubility in CO₂, nonionic surfactants have become a research hotspot for CO₂ gas-soluble surfactants. Xing et al.^[161] studied some nonionic surfactants, including alkylphenol ethoxylates, alkyl ethoxylates, and fatty acid-based surfactants. They found that most of these surfactants were soluble in CO₂ in the range of 0.02%–0.06% at 1500 psia and 25°C, with a certain ability to stabilize foam. The foam produced by branched alkylphenol ethoxylates is the most stable. The emulsions generated by surfactants with longer ethoxylated chains had more droplets and a wider size distribution than their analogs with shorter ethoxylated chains. Bi et al.^[31] found that the foaming volume and half-life of CO₂ foams increased with increasing the number of EO groups (polyoxyethylene groups) in a single molecule of the kind of alkylphenol ethoxylate surfactants. They also found that these surfactants can stabilize CO₂ in 5wt% NaCl brine emulsion^[25]. Therefore, when the continuously injected CO₂/surfactant solution is mixed with the formation brine, emulsion or foam may be formed in the reservoir, thus avoiding or reducing the necessity of alternating injection of surfactant aqueous solution during CO₂ injection. Notably, the π – π stacking of the benzene ring can enhance surfactant stacking at the CO₂-brine interface and stabilize the water film, resulting in a more stable emulsion generated by alkylphenol ethoxylates than by branched alkyl ethoxylates.

Surfactants, such as alkylphenol ethoxylates or alkyl ethoxylates, have been extensively examined as effective C/W foaming agents at medium and low temperatures (6, 9, and 10°C). However, at high temperatures, they readily precipitate and the hydrogen bonds between EO groups and water are weakened broken, resulting in solvent loss^[174–176]. Bi et al.^[31] revealed that alkylphenol ethoxylate sulfonates obtained by the sulfonation of alkylphenol ethoxylate ethers produced CO₂ foam with certain stability at 125°C, with a half-life of 6.54 min. Surfactant hydrophilicity was enhanced after sulfonation, resulting in excellent foam stability. This approach also produced stable CO₂ foam at higher temperatures, and the foaming ability, foam stability, and temperature resistance

of these surfactants were significantly improved. McLendon et al.^[177] found that the alkyl chain of the DOW Tergitol NP Series remained unchanged as the polyethylene glycol increased from nine ethylene oxide groups to 12 ethylene oxide groups. The CO₂-philic polyethylene glycol chains increased, but the CO₂-phobic hydroxyl groups remained unchanged, resulting in more CO₂-philic and hydrophilic molecules. In addition, foam cloud point pressure decreased, while the surfactant became more soluble in CO₂. At a very dilute concentration with approximately 0.10% solubility, branched or linear hydrocarbon tails seemed to have a negligible effect on the CO₂ solubility of surfactants. Foad et al.^[30] studied wettability and found that SURFONIC® N-100 (0.1wt%) significantly enhanced CO₂ ability to change the sample wettability, from medium to wet, with a water-shale-air contact angle reduced from 118° to 36°.

3.2.2. Ionic Surfactants

Although ionic surfactants may have potentially high cloud point pressures compared to nonionic surfactants, most ionic surfactants have very limited solubility in CO₂^[178]. This is because supercritical CO₂ is a non-polar solvent, while ionic surfactants have polar head groups, which leads to poor solubility in non-polar solvents. Some ionic surfactants with CO₂ solubility developed after years of research.

Sodium alkyl sulfate anionic surfactant has a certain solubility in CO₂. It can produce CO₂ foam with a certain stability at 125°C, and the half-life is about 7.39 min^[31]. Under normal conditions, there is no direct dissolution between carbon dioxide and sodium alkyl sulfate. Under supercritical conditions, sodium alkyl sulfate can dissolve in supercritical carbon dioxide. Although anionic surfactants can improve foam stability at lower water saturation compared with nonionic surfactants, thereby reducing residual water saturation and increasing the pore volume of CO₂ storage^[179], their applications also have limitations. They are highly adsorbed on the carbonate surface^[180], and some precipitate in hard water or high salt brine^[181,182]. Xue et al.^[23] studied a sulfonate head-based anion surfactant and found that the surfactant could dissolve in CO₂ and form stable viscous C/W foam at high salinity (14.6% TDS) and high temperature (120°C). Viscous foam can still form after CO₂ is diluted by 20% methane. The presence of high salt concentrations, especially divalent salts, will inevitably lead to the screening of electrostatic interactions between the surfactant head group and mineral surface^[183]. Divalent cations can bridge the surfactant head group and mineral surface^[184]. Anionic surfactants are usually used in sandstone reservoirs to minimize adsorption. However, various sulfate-containing anionic surfactants are prone to hydrolysis under high temperature acidic conditions with pH < 4 in sandstone reservoirs in the presence of CO₂^[185].

Compared with anionic surfactants, cationic surfactants can significantly reduce the adsorption of surfactant components on the surface of carbonates^[56]. Cationic surfactants, such as ethoxyamine surfactants, have good solubility and stability in high temperature and high salt brine, but they are often adsorbed on negatively charged sandstone reservoirs due to electrostatic attraction^[186]. The study found that ethoxylated cocoamines can dissolve in CO₂ and form CO₂ foam under high temperature (120°C), high pressure (3400 psi), and high salinity (22% TDS), which effectively reduces fluidity. However, the minimum pressure gradient requires a higher injection rate. A lower injection rate is then required to produce stronger foam due to the shear-thinning effect. Notably, the adsorption capacity of carbonate formation (0.10–0.13 mg/m²) is low^[186,187]. Although cationic surfactants have good solubility and foaming properties at high temperatures, quaternary ammonium salts are prone to thermal degradation at high temperatures^[188,189]. Chen et al.^[190] optimized the tail length of trimethyl ammonium cationic surfactant and found that the optimized surfactant can be effectively dissolved in brine with 22% TDS at 120°C. It can achieve high surfactant adsorption at the CO₂–water interface (area/surfactant molecule 154Å²), and the interfacial tension is reduced from about 40 mN/m to about 6 mN/m. The above properties make the apparent viscosity of C/W foam at 120°C to be 14 mPa•s, which is stable in both the crushed calcium carbonate packed bed (75 µm²) and the capillary downstream of the bed. In addition, the partition coefficient of surfactant between oil and 22% TDS (255 kg/m³) brine is less than 0.15, which will help minimize the loss of surfactant in the oil phase in applications such as EOR and hydraulic fracturing.

Zwitterionic surfactant is a surfactant formed by connecting one or two head groups of surfactants near the hydrophilic head group or hydrophilic head group through a chemical bond. Cocoyl amide propyldimethyl glycine can produce CO₂ foam with certain stability at a high temperature (125°C), and the half-life is about 24.96 min. Its foaming performance is good, but the adsorption capacity in the formation is higher^[31]. AlYousef et al.^[165] found that lauroylamide propylbetaine effectively stabilized the foam at 100°C, 2000 psi, and >57,000 ppm salt water salinity. The apparent viscosity of the foam was high. With decreased foam quality, the foam viscosity increased. The adsorption experiment results showed that the injected surfactant solution had a recovery rate of 86.56%. Notably, the amount of surfactant adsorbed by rock is about 0.257 mg/g rock, and the adsorption amount of rock is small. Zhou et al.^[191] found that the adsorption amount of cocoyl amide propyldimethyl glycine in carbonate was lower (1 mg/g rock) than that in sandstone. Xue et al.^[123] studied the N-dodecyl-N, N-dimethyl-3-ammonio-1-propanesulfonate and found that the surfactant dissolved in CO₂ and stabilized the viscous C/W foam at high temperature (120°C) and high salinity (14.6% TDS) salt water, even when CO₂ is diluted by 20% methane.

3.2.3. Fluorine- and Nitrogen-Containing Surfactants

Due to their superior performance, fluorine- and nitrogen-containing surfactants have been the subject of numerous studies in the earliest research on CO₂-soluble surfactants. Marcio et al.^[192] experimentally demonstrated the interaction between fluorine atoms and CO₂ molecules. According to the Lewis acid–base theory, they considered fluorine to be a Lewis base and carbon in CO₂ to be a Lewis acid. By preparing W/C microemulsion with fluorinated AOT homolog surfactants, Eastoe et al.^[193] found that the structure of fluorinated surfactants had a significant effect on the microemulsion's stability. They believed that the fluorine atom can shield fluorocarbon chains well because it has a higher radius than the hydrogen atom. Moreover, the low cohesive energy density, solubility parameter, and polarization ability of fluorinated chains make fluorocarbon chains more compatible with CO₂. Therefore, fluorinated surfactants can act well on the water–CO₂ interface and have high surface activity. Eastoe et al.^[194] studied the W/C stability of various fluorine-containing AOT homologs to better elucidate the relationship between the structure and properties of these homologs. These surfactants have two tail chains with different fluorination degrees, and the perfluorinated tail chain plays an important role in stabilizing the W/C microemulsion. The main reasons for the good solubility of fluorinated surfactants in CO₂ are summarized as follows^[166]: (1) The cohesive energy density of fluorine-containing surfactants is small. The presence of fluorine atoms can reduce the interaction force between surfactants. (2) Fluorine atoms with high electronegativity can interact with carbon atoms in CO₂ to increase the interaction force between surfactants and CO₂. The flexibility of the fluorinated chain is better and the glass transition temperature is lower. (3) The presence of fluorine affects the acidity of adjacent protons, resulting in specific interactions between these protons and the oxygen atoms of CO₂. Furthermore, silicon-containing surfactants have high surface activity similar to fluorine-containing surfactants. Silicon-containing molecular chains have good flexibility, low glass transition temperature, and cohesive energy density, in addition to small intramolecular interactions that facilitate the dissolution of siloxane polymers in CO₂^[195]. Beckman^[166] synthesized two functional silicones based on previous studies. The difference in the functional silicones is the carbonyl group on the side chain. They found that adding a carbonyl group to silicon-containing alkyl side chains can greatly improve the solubility of functional silicones. Carbonyl group addition reduces the intermolecular force of functional silicone and improves surfactant solubility. In this case, CO₂ as the Lewis acid reacts closely with the carbonyl group as the Lewis base. Fink et al.^[166,167] synthesized polyoxyethylene and polyoxypropylene silicon-containing functional surfactants to better explain the effect of oxygen-containing functional groups on the solubility of silicon-containing polymers in CO₂. They found that these surfactants have good solubility in CO₂ and that surfactants with less ethylene oxide addition or less polyoxyethylene propylene chain have better solubility. Low-molecular-weight polyoxyethylene silicon-containing surfactants have a smaller cloud point pressure than high

molecular weight polyoxyethylene silicon-containing surfactants. They believe that the polar chain influences solubility more than the molecular weight.

3.2.4. Surfactant Blended Systems

A mixed surfactant is a surfactant system comprising several surfactants that are mixed with other surfactants as agents^[198]. The study of water-soluble surfactants showed that the mixture synergistically exhibited better foaming properties than a single surfactant, improving foam stability and reducing crude oil instability. However, some mixed surfactants form crystalline precipitates in aqueous solutions due to the Coulomb interaction between oppositely charged substances^[170]. The mixed surfactant system is also severely limited by CO₂ solubility. Nicolas et al.^[171] mixed cationic surfactant F-CAT with anionic surfactant F-OPT, which reduced the static adsorption of surfactant in carbonate reservoirs and significantly improved the apparent viscosity in the presence of oil. The apparent viscosity is mainly determined by the CO₂ density value, not the temperature, even at different temperatures. It differs from nondense gas foams. Mixed surfactant foams have higher stability and viscosity than single surfactant foams, regardless of the presence of oil. This is mainly due to the close packing of surfactant layers at the gas-liquid interface, which has strong viscoelasticity and leads to higher separation pressure. Zhang et al.^[173] studied the synergistic effect of a CO₂-soluble surfactant mixture comprising an ethoxylamine head group (C₁₂NEO₂) with two coconut oil alkyl tails and a highly ethoxylated nonionic surfactant (C₁₃EO₁₂). They found that adding C₁₃EO₁₂ to C₁₂NEO₂ resulted in lower CMC and negative interaction parameter β^σ . It showed a positive synergistic effect. Although C₁₃EO₁₂ was difficult to dissolve in CO₂ alone, the 0.2wt% surfactant mixture (C₁₃EO₁₂ ratio is less than 30%) was completely soluble in CO₂ at 60°C and 16 MPa to form a transparent single phase. The best surfactant ratio was C₁₂NEO₂:C₁₃EO₁₂ = 8:2. The volume foam stability and viscosity increased 1.5 times and 2.5 times, respectively. The combined surfactant solution has greater solubility in CO₂ than a single CO₂-soluble surfactant and can further improve foam viscosity.

4. Conclusions and Future Outlook

Their synergistic effect with CO₂ can enhance oil recovery more effectively. The application and storage of CO₂ in oil reservoirs can also effectively alleviate the increase in CO₂ concentration in the atmosphere and reduce the greenhouse effect. Therefore, CO₂-soluble surfactants have broad application prospects in oilfield development and have attracted much attention. However, other issues still exist that require additional research.

(1) A CO₂-soluble surfactant system is divided into CO₂ + surfactant (+ agents) and CO₂ + surfactant (+agents) + water. Notably, adding agents and water aids in increasing CO₂ ability to carry surfactants. Continuous injection is more economical and has great potential. The macro-phase behavior of surfactant, water, and CO₂ was judged by cloud point pressure in the static experiment to determine the foam stability and solubilization performance of the microemulsion. The foaming performance was then evaluated based on foam volume and foam half-life. The dynamic experimental evaluation method was used to analyze the sealing ability of foam based on the resistance coefficient and residual resistance factor. While CO₂ can form miscible flooding with crude oil, gas-soluble surfactants can effectively reduce the miscible pressure. Therefore, the interfacial properties can be measured using the hanging drop method to analyze changes in miscible pressure.

(2) Snap-off, lamellar division, and leave-behind are the three mechanisms that generate foam in porous media. Foam coalescence is generally due to capillary suction and gas diffusion. Capillary suction is widely considered the main mechanism of foam rupture. Empirical or semi-empirical and mechanical models (population balance models) can analyze foam fluidity. Empirical or semi-empirical models are more targeted, whereas mechanical models are more universal. Although many studies have explored foam performance under different conditions and the improvement of foam mobility models, research on CO₂-soluble surfactants must be combined with effective on-site cases to provide more valuable information for future development.

(3) CO₂ foam can effectively improve the sweep range and oil displacement efficiency of CO₂ by reducing the oil–gas mobility ratio, selective plugging, and reducing interfacial tension to change rock wettability. Retention foam can prolong the contact time between CO₂ and oil, resulting in a better CO₂ flooding mechanism. However, the study of minimum miscible pressure reduction in the CO₂–oil system with gas-soluble surfactants remains in the exploratory stage. Many issues need to be addressed. For instance, as the mechanism of agents in the system is not sufficiently evident, improving the interaction mechanism between CO₂, surfactants, agents, and oil is highly desirable.

(4) Surfactant solubility in CO₂ is the primary parameter for screening CO₂-soluble surfactants, followed by the analysis of foam properties, thermal stability, and adsorption behavior. At present, only a few CO₂-philic surfactants exist. Although fluorine- and silicon-containing surfactants have high surface activity, small cohesive energy, and good compatibility with CO₂, difficult degradation, high toxicity, and high cost seriously limit their field applications. The existing CO₂-philic hydrocarbon surfactants are affordable, but their solubility in CO₂ is small, with limited foam performance. Many current studies focus on nonionic surfactants. Anionic, cationic, and zwitterionic surfactants, as well as two or more mixed surfactants, have also been studied, although their overall foaming performance requires further improvement. Overall, enhancing the foam performance of nonionic surfactants or improving the solubility of ionic surfactants in CO₂ will be effective in realizing improved oil recovery efficiency.

(5) This article explores the application of CO₂ soluble surfactants in tight reservoirs with low permeability and high reservoir heterogeneity. Advanced screening and simulation techniques are introduced to more accurately predict the behavior of surfactants in reservoirs, reducing the time and cost of experimental stages.

(6) Future research should focus on developing new CO₂-soluble surfactants that address current limitations while enhancing performance in challenging reservoir conditions. One promising direction is the development of environmentally friendly and biodegradable surfactants. With increasing environmental regulations and the need for sustainable oil recovery methods, the use of green chemistry to design surfactants that are both highly effective and environmentally benign will become critical. Additionally, fluorinated surfactants and siloxane-based surfactants have shown potential for improving solubility and stability in supercritical CO₂, especially under high temperature and salinity conditions. Research could also explore the development of nanoparticle-enhanced surfactants, which combine the stability of nanoparticles with surfactant-based foam systems to further increase foam stability and extend the duration of mobility control. Another promising direction is the customization of surfactant molecular structures to target specific reservoir characteristics. For example, surfactants with branched or double-tail hydro-phobic groups could be designed to improve solubility in CO₂, while introducing functional groups that enhance interactions with formation water could lead to more stable foam films in highly heterogeneous or low-permeability reservoirs.

Acknowledgments: This work was supported by the Heilongjiang Provincial Natural Science Foundation of Joint Guidance Project (Grant No. LH2022E022), the Major Science and Technology Projects of PetroChina (Grant No.2021ZZ01-08).

References

1. Wang,F.S., Mou,Z.B., Liu,P.C., Zhang,S.F., Wang,C., Li,X.L. Experiment and numerical simulation on mechanism of CO₂ assisted mining in super heavy oil reservoirs.*Petroleum Geology and Recovery Efficiency*, 2017, 24(6): 86-91.
2. Hamouda,A. A., Chughtai,S.Miscible CO₂ flooding for EOR in the presence of natural gas components in displacing and displaced fluids. *Energies*, 2018, 11(2): 391.
3. Liu,L.C., Li,Q., Zhang,J.T., Cao,D. Toward a framework of environmental risk management for CO₂ geological storage in China: gaps and suggestions for future regulations. *Mitig Adapt Strategies Global Change*, 2016,21(2):191–207.
4. Guo, F., & Aryana, S. A. Improved sweep efficiency due to foam flooding in a heterogeneous microfluidic device. *Journal of Petroleum Science and Engineering*, 2018,164, 155-163.

5. Jin, F., Chen, S., Wei, B., Wang, D., Yang, W., Wang, Y., & Lu, J. Visualization of CO₂ foam generation, propagation and sweep in a complex 2D heterogeneous fracture network. *Fuel*, 2021,302, 121000.
6. Wang,Y.C., Zhao,Z.D.Experimental Research on the Effect of Pressure on CO₂ Oil Displacement Efficiency. *Special Oil & Gas Reservoirs*, 2017, 24(4): 132-135.
7. Mathew,E. S., Shaik,A. R., Sumaiti,A.A., AlAmeri,W. Effect of oil presence on CO₂ foam based mobility control in high temperature high salinity carbonate reservoirs. *Energy Fuels*, 2018, 32(3): 2983 - 2992.
8. Sie,C.Y., Nguyen,Q.P. A non-aqueous foam concept for improving hydrocarbon miscible flooding in low permeability oil formations. *Fuel*, 2021, 288(2):119732.
9. Zhang Y , Wang, Y.T. , Xue, F.F. , Wang, Y.Q., Ren, B. , Zhang, L.Ren,S.R. CO₂ foam flooding for improved oil recovery: Reservoir simulation models and influencing factors. *Journal of Petroleum Science & Engineering*, 2015,133:838-850
10. Li S, Yang K, Li Z, et al. Properties of CO₂ foam stabilized by hydrophilic nanoparticles and nonionic surfactants. *Energy & Fuels*, 2019, 33(6): 5043-5054.
11. Liang S, Luo W, Luo Z, et al. Research of CO₂-Soluble Surfactants for Enhanced Oil Recovery: Review and Outlook. *Molecules*, 2023, 28(24): 8042.
12. Hosseini, H., Tsau, J. S., Wasserbauer, J., Aryana, S. A., & Ghahfarokhi, R. B. Synergistic foam stabilization and transport improvement in simulated fractures with polyelectrolyte complex nanoparticles: Microscale observation using laser etched glass micromodels. *Fuel*, 2021, 301, 121004.
13. Song,Y.X.,Zhou,Y.X.,Zhang,W.M.Application of foam fluid in oil field.Foreign Oilfield Engineering, 1997: 13(1): 5-8.
14. Li,Z.L.,Qian,W.D.An overview of application of foam fluid in oil fields in China.Oil Drilling & Production Technology, 1993, 15(6): 88-94.
15. Yu,Q.T.On Research Strategy for Enhancing Oil Recovery Factor. *Xinjiang Petroleum Geology*, 2000, 21(4): 307-310.
16. Liu,Z.K, Min,J.H. Application of Foam Flooding in Shengli Oil Field. *Oil & Gas Recovery Technology*, 1996, 3(3): 24-29.
17. Beyer A. H., Millhone R. S., Foote R. W. Flow behavior of foam as a well circulating fluid.In: *the Fall Meeting of the Society of Petroleum Engineers of AIME*, San Antonio, Texas, 1972.
18. Blauer R. E., Kohlhaas C. A. Formation fracturing with foam.In: *the Fall Meeting of the Society of Petroleum Engineers of AIME*, Houston, Texas, 1974.
19. Stone H. L., Vertical, Conformance In An Alternating Water-Miscible Gas Flood. In: *the SPE Annual Technical Conference and Exhibition*, New Orleans, Louisiana, 1982.
20. Righi, E. F., Royo, J., Gentil, P., Castelo, R., Bosco, S. Experimental study of tertiary immiscible WAG injection.In: *the SPE/DOE Symposium on Improved Oil Recovery*, Tulsa, Oklahoma, 2004.
21. Lawson J. B., The adsorption of non-ionic and anionic surfactants on sandstone and carbonate.In:*SPE Symposium on Improved Methods of Oil Recovery*. Tulsa, Oklahoma,1978.
22. Zhao,Y.P.,Zhao,X.S.,Li,J.Yao,Z.J.,Zhao,Y.Indoor Experiment And Field Application Of CO₂ Flooding In Ultra-Low Permeability Oil Reservoirs.*Petroleum Geology & Oilfield Development in Daqing*, 2018, 37(1): 128-133.
23. Xue,Z., Panthi, K., Fei,Y.P., Johnston,K.P., Mohanty,K.K. CO₂-Soluble Ionic Surfactants and CO₂ Foams for High-Temperature and High-Salinity Sandstone Reservoirs. *Energy Fuels*, 2015, 29(9): 5750-5760.
24. Le, V. Q. , Nguyen, Q. P. , Sanders, A. A novel foam concept with CO₂ dissolved surfactants. In: *the SPE Symposium on Improved Oil Recovery*, Tulsa, Oklahoma, USA, 2008.
25. Xing,D.Z., Wei,B., Trickett,K., Mohamed,A., Eastoe,J, Soong,Y., Enick,R. CO₂-soluble surfactants for improved mobility control.In: *the SPE Improved Oil Recovery Symposium*, Tulsa, Oklahoma, USA, 2010.
26. Zhu,Z.Q. Supercritical Fluid Technology - Principles and Applications. *Book Published by the China Chemical Industry Press*, Beijing,China,2000.
27. Han,B.X. Supercritical Fluid Science and Technology. *Book Published by the China Petrochemical Press*, Beijing,China,2005.
28. Zhang C.Research on Stabilization Mechanism and Flow Characteristics of CO₂ Foam on the Basis of Gas-soluble Surfactant. *Dissertation*,China University of Petroleum,2016
29. Bond, D.C. Method for recovering oil from subterranean formations. *US Patent 3342261*, 1967.
30. Haeri, F., Burrows, L. , Lemaire, P. , Shah, P. G. , Tapriyal,D., Enick,R.M., Crandall,D.M., Goodman, A. Improving CO₂-EOR In Shale Reservoirs using Dilute Concentrations of Wettability-Altering CO₂-Soluble Nonionic Surfactants.In: *the SPE/AAPG/SEG Unconventional Resources Technology Conference*, Virtual, 2020.
31. Bi,W.Y.Development and performance evaluation on CO₂-soluble surfactant foam system for low permeability reservoir.*Petroleum Geology and Recovery Efficiency*, 2018, 25(6): 71-77.
32. Raveendran P., Shervani Z., Ikushima, Y., Liu J. Micellization of sodium bis (2-ethylhexyl) sulfosuccinate in supercritical CO₂ with fluorinated co-surfactant and its solubilization of hydrophilic species. *Journal of Supercritical Fluids*, 2005, 33(2): 121-130.

33. Johnston K. P., Harrison K. L., Clarke M. J., Howdle, S. M., Heitz, M. P., Bright, F. V., CARLIER, C., Randolph, T. W.. Water-in-carbon dioxide microemulsions: an environment for hydrophiles including proteins. *Science*, 1996, 271(5249): 624-626.
34. Cui, Bo., Dong, Z.X., Li, Y., Lin, M.Q. Cloud Point Pressure of Supercritical Carbon Dioxide Microemulsion System. *Petrochemical Technology*, 2013, 42(3): 303-307.
35. Liu, J.C., Han, B.X., Zhang, J.L., Mu, T.C., Li, G.Z., Wu, W.Z., Yang, G.Y. Effect of cosolvent on the phase behavior of non-fluorous Ls-54 surfactant in supercritical CO₂. *Fluid phase equilibria*, 2003, 211(2): 265-271.
36. Patzek T. W. Field Application of Foam for Mobility Improvement and Profile Control. *SPE Res. Eng.*, 1996, 11(2): 79-85.
37. Zhang, Y.H. Gas Solubility and Plugging Performance of CO₂-soluble Foaming Agent. *Science Technology and Engineering*, 2017, 21(17): 1671-1815.
38. Wei, X. Study on visualized foaming properties of CO₂ gas soluble foaming agent. *Advances in Fine Petrochemicals*, 2021, 22(1): 33-35.
39. Cheng, X.F., Feng, C.G., Wang, Y., Wang, L.Q., Wang, F.L. Study on Solvent Characteristics of Active Composition of Herbs in SCF-CO₂. *Chemistry*, 2000, 3(1): 26-29.
40. Committee O. EOR laboratory evaluation method for steam foam injection SY/T 6955-2013. Beijing: China Standard Press, 2013.
41. Pang, Z.X., Wu, Y.L., Zhao M. Novel Evaluation Method of Foam Agents for Thermal Recovery in Heavy Oil Reservoirs. *Energy Fuels*, 2016, 30(4): 2948-2957.
42. Hutchinson D. A., Demiral B. D. M., Castanier L. Steam Foam Studies In The Presence of Residual Oil. In: *the SPE Latin America Petroleum Engineering Conference*, Caracas, Venezuela, 1992.
43. Luo, H., Zhang, Y.C., Fan, W.Y., Nan, G.Z., Li, Z.M. Effects of the non-ionic surfactant (CiPOj) on the interfacial tension behavior between CO₂ and crude oil. *Energy Fuels*, 2018, 32(6): 6708-6712.
44. Farajzadeh, R., Lopez-Salinas, J. L., Miller, C. A., Biswal, S. L., Hirasaki, G. J. Estimation of Parameters for the Simulation of Foam Flow through Porous Media. Part1: The Dry-Out Effect. *Energy Fuels*, 2013, 27(5): 2363-2375.
45. Alvarez J. M., Rivas H. J., Rossen W. R. Unified Model for Steady-State Foam Behavior at High and Low Foam Qualities. *SPE J.*, 2001, 6(3): 325-333.
46. Khatib Z. I., Hirasaki G. J., Falls A. H. Effects of Capillary Pressure on Coalescence and Phase Mobilities in Foams Flowing Through Porous Media. *SPE Res. Eval. & Eng.*, 1988, 3(3): 919-926.
47. Rossen W. R., Wang M. W. Modeling Foams for Acid Diversion. *SPE J.*, 1999, 4(2): 92-100.
48. Kraynik, A.M., Reinelt D.A., Sivarajan, S. Rheology of Foams. *Materials Science and Materials Engineering*, 2018.
49. Hutchins R. D., Miller M. J., A Circulating Foam Loop for Evaluating Foam at Conditions of Use. *SPE Prod & Fac.*, 2005, 20 (4): 286-294.
50. Alexander, S., Barron, A. R., Denkov, N., Grassia, P., Kiani, S., Sagisaka, M., ... & Shokri, N. Foam generation and stability: role of the surfactant structure and asphaltene aggregates. *Industrial & Engineering Chemistry Research*, 2021, 61(1), 372-381.
51. Orujov, A., Coddington, K., & Aryana, S. A. A review of CCUS in the context of foams, regulatory frameworks and monitoring. *Energies*, 2023, 16(7), 3284.
52. Falls A.H., Hirasaki G.J., Patzek T.W., Gauglitz, D.A., Miller, D.D., Ratulowski, T. Development of a mechanistic Foam Simulator: The Population Balance and Generation by Snap-Off. *SPE Res. Eng.*, 1988, 3(3): 884-892.
53. Boud D. C., Holbrook O. C. Gas drive oil recovery process: US 2866507, 1958.
54. Nguyen, Q., Alexandrov, A., Zitha, P., & Currie, P. Experimental and Modeling Studies on Foam in Porous Media: A Review. In: *the SPE International Symposium on Formation Damage Control*, Lafayette, Louisiana, 2000.
55. Hirasaki G. J., Lawson J. B. Mechanisms of Foam Flow in Porous Media: Apparent Viscosity in Smooth Capillaries. *Society of Petroleum Engineers*. 1985, 25(2), 176-190.
56. Hahn, R.E. Novel Cationic Surfactants for CO₂-Foam Flooding in Carbonate Reservoirs. *Dissertation*, the University of Texas at Austin, 2015.
57. Delamaide E., Cuenca A., Chabert M. State of the Art Review of the Steam Foam Process. In: *at the SPE Latin America and Caribbean Heavy and Extra Heavy Oil Conference*, Lima, Peru, 2016.
58. Cui L.Y., Ma, K., Puerto, M., Abdala, A.A., Tanakov, I., Lu, L.J., Chen, Y.S., Elhag, A., Johnston, K.P., Biswal, S.L. Mobility of ethomeen C12 and carbon dioxide (CO₂) foam at high temperature/high salinity and in carbonate core. *SPE J.*, 2016; 21(4): 1151-1163.
59. Friedmann F., Chen W. H., Gauglitz P. A. Experimental and Simulation Study of High-Temperature Foam Displacement in Porous Media. *SPE Res. Eng.*, 1991, 6(1): 37-45.
60. Kovscek A. R., Radke C. J. Fundamentals of Foam Transport in Porous Media. *Foams: Fundamentals and Applications in the Petroleum Industry. American Chemical Society*, 1994. 242: 115-163.

61. Schramm L.L. Foams: Fundamentals and Applications in the Petroleum Industry. Laurier L. Schramm (Petroleum Research Institute). American Chemical Society: Washington, DC, 1994.
62. de Azevedo, B. R. S., Alvarenga, B. G., Percebom, A. M., & Pérez-Gramatges, A. Interplay of interfacial and rheological properties on drainage reduction in CO₂ foam stabilised by surfactant/nanoparticle mixtures in brine. *Colloids and Interfaces*, 2023,7(1), 2.
63. Guo, F., & Aryana, S. An experimental investigation of nanoparticle-stabilized CO₂ foam used in enhanced oil recovery. *Fuel*, 2016,186, 430-442.
64. Guo, F., He, J., Johnson, P. A., & Aryana, S. A. Stabilization of CO₂ foam using by-product fly ash and recyclable iron oxide nanoparticles to improve carbon utilization in EOR processes. *Sustainable Energy & Fuels*, 2017,1(4), 814-822.
65. Almajid M., Kovscek A., Pore-level mechanics of foam generation and coalescence in the presence of oil. *Advances in Colloid and Interface Science*, 2016, 233: 65-82.
66. Farajzadeh R., Andrianov A., Zitha P. Investigation of Immiscible and Miscible Foam for Enhancing Oil Recovery. *Industrial & Engineering Chemistry Research*, 2010, 49(4):1910-1919.
67. Rossen W. R., Gauglitz P. A. Percolation Theory of Creation and Mobilization of Foams in Porous Media. *AIChE Journal*, 1990, 36(8): 1176-1188.
68. Consan K. A., Smith R. D. Observations on the solubility of surfactants and related molecules in carbon dioxide at 50°C. *J. Supercrit Fluids*, 1990, 3(2): 51-65.
69. Hoeffling, T. A. , Beitle, R. R. , Enick, R. M. , Beckman, E. J. Design and synthesis of highly CO₂-soluble surfactants and chelating agents. *Fluid Phase Equilib*, 1993, 83(2): 203-212.
70. Eastoe J., Gold S. Self-assembly in green solvents. *Phys.Chem. Chem. Phys.*, 2005, 7(7): 1352-1362.
71. Desimone J. M., Keiper J. S., Surfactants and self-assembly in carbon dioxide. *Curr Opin Solid State Mater Sci.*, 2001, 5(4): 333-341.
72. Fan X., Potluri V. K., Mcleod M. C., Wang,Y.,Liu,J.C., Enick,R.M., Hamilton,A.D., Roberts,C.B, Johnson,J.K., Beckman,E.J. Oxygenated hydrocarbon ionic surfactants exhibit CO₂ solubility. *J.Am.Chem.Soc.*, 2005, 127(33): 11754-11762.
73. Liu,J.C., Han B.X., Wang,Z.W.,Zhang,J.L.,Li,G.Z.,Yang,G.Y. Solubility of Ls-36 and Ls-45 surfactants in supercritical CO₂ and loading water in the CO₂/water/surfactant systems. *Langmuir*, 2002, 18(8): 3086-3089.
74. Sandro R. P. da Rocha, Kristi L. Harrison, Keith P. Johnston. Effect of surfactants on the interfacial tension and emulsion formation between water and carbon dioxide. *Langmuir*, 1999, 15(2): 419-428.
75. Sagisaka, M. , Fujii, T. , Koike, D. , Yoda, S. , Takebayashi, Y. , Furuya, T, Yoshizawa,A., Sakai,H., Abe,M., Otake,K. Surfactant-mixing effects on the interfacial tension and the microemulsion formation in water/supercritical CO₂ system. *Langmuir*, 2007, 23(5): 2369-2375.
76. Sagisaka M., Koike D., Mashimo Y., Yoda, S., Takebayashi, Y., Furuya, T. Yoshizawa,A., Sakai,H., Abe,M., Otake,K. Water/supercritical CO₂ microemulsions with mixed surfactant systems[J]. *Langmuir*, 2008, 24(18): 10116-10122.
77. Li,G.Z.,Guo,R. Theory and Application of micro emulsion. *Book Published by the China Petroleum Industry Press*, Beijing,China,1995.
78. Clarke, M. J. , Harrison, K. L., Johnston, K. P. Water in Supercritical Carbon Dioxide Microemulsions: Spectroscopic Investigation of a New Environment for Aqueous Inorganic Chemistry. *Journal of the American Chemical Society*, 1997,119(27):6399-6406.
79. Hutton, B. H. , Perera, J. M. , Grieser, F. , Stevens, G. W. AOT reverse microemulsions in sc CO₂-a further investigation. *Colloids and surfaces A: Physicochemical and engineering aspects*, 2001, 189(1-3): 177-181.
80. Singley E. J., Liu W., Beckman E. J. Phase behavior and emulsion formation of novel fluoroether amphiphiles in carbon dioxide. *Fluid Phase Equilibria*, 1997, 128(1): 199-219.
81. Gao,B.J..Application for solubility parameter. *Shanxi Chemical Industry*, 1998, 2: 18-19.
82. Majer V., Svoboda V., Pick J., Heats of Vaporization of Fluids. *Book Published by the Elsevier, Amsterdam, Oxford, New York, Tokyo*,1989.
83. Huang,X.H.Relationship between solvent selection and solubility parameters of recrystallization. *Chemistry Online*, 1999, 1(1): 35-38.
84. Sambasiva R. A. Solubility Parameters of Supercritical Fluids. *Ind. Eng. Chem. Process Des. Dev.*, 1984, 23 (2): 344-348.
85. Vimon T., Nimit W., Wibul W., Prediction of solubility parameters using partial least square regression . *International Journal of Pharmaceutics*, 2006, 325 (1-2): 8-14.
86. Xia,Q.,Yin,K.L.Calculation of Solubility Parameters of Organic Solvents by Molecular Dynamics Simulation. *Journal of Jiangsu Polytechnic University*, 2004, 16(1): 40-42.
87. Zhang,C., Li,Z.M., Li,S.Y, Lv,Q.C.,Wang,P.,Liu,J.Q,Liu,J.L. Enhancing sodium bis (2-ethylhexyl) sulfosuccinate injectivity for CO₂ foam formation in low-permeability cores: Dissolving in CO₂ with ethanol. *Energy Fuels*, 2018, 32(5): 5846-5856.
88. Yang,Z.H, Liu,X.L., Hua,Z., Ling,Y.,Li,M.Y.,Lin,M.Q.,Dong,Z.X. Interfacial tension of CO₂ and crude oils under high pressure and temperature. *Colloids Surf.A: Physicochem Eng Aspects*, 2015, 482: 611-616.

89. Dong M.Z, Huang S., Dyer S. B., Mourits,F.M. A comparison of CO₂ minimum miscibility pressure determinations for Weyburn crude oil. *J.Pet.Sci.Eng.*, 2001, 31(1): 13-22.
90. Yang, Z.H., Li, M.Y., Peng, B. , Lin, M.Q., Dong, Z.X.,Ling, Y. Interfacial tension of CO₂ and organic liquid under high pressure and temperature. *Chinese Journal of Chemical Engineering*, 2014, 22(11/12): 1302-1306.
91. Talebian S. H., Masoudi R., Tan, I. M. , & Zitha, P. Foam assisted CO₂-EOR: A review of concept, challenges, and future prospects. *J. Pet. Sci. Eng.*, 2014, 120: 202-215.
92. Radke C. J., Ransohoff T., Mechanism of Foam Generation in Glass-Bead Packs[M]. 1986. 3.
93. Kovscek A., Radke C. Gas bubble snap-off under pressure-driven flow in constricted noncircular capillaries. *Colloids and Surfaces A: Physicochemical and Engineering Aspects*, 1996, 117(1-2): 55-76.
94. Chambers K.T., Radke C.J. Capillary Phenomena in Foam Flow Through Porous Media in Interfacial Phenomena in Petroleum Recovery, *Publisher: Marcel Dekker, Inc.* Editors: Morrow, N. R.,1990: 191-255.
95. Almajid M.M., Kovscek A.R. Pore Network Investigation of Trapped Gas and Foam Generation Mechanisms. *Transp Porous Media*, 2020, 131: 289-313.
96. Langevin D. Bubble coalescence in pure liquids and in surfactant solutions. *Current Opinion in Colloid & Interface Science*, 2015, 20(2): 92–97.
97. Pugh R. J. Foaming, foam films, antifoaming and defoaming. *Advances in Colloid and Interface Science*, 1996, 64: 67–142.
98. Huang D. D., Nikolov A., Wasan D. T., Foams: basic properties with application to porous media. *Langmuir*, 1986, 2(5): 672–677.
99. Kapetas, L. , Bonnieu, S. V. , Danelis, S. , Rossen, W. R. , Farajzadeh, R. , & Eftekhari, A. A. Shafian,S.R.M., Bahrim,R.Z.K. Effect of Temperature on Foam Flow in Porous Media. *Journal of Industrial & Engineering Chemistry*, 2016,36:229-237.
100. Farajzadeh, R., Andrianov, A., Krastev, R., Hirasaki, G. , Rossen, W. R. Foam-Oil interaction in porous media: Implications for foam assisted enhanced oil recovery. In: *the SPE EOR Conference at Oil and Gas West Asia*, Muscat, Oman, 2012.
101. Chen Y., Elhag A. S., Poon B. M., Cui, L. , Ma, K. ,Liao, S. Y. , Omar,A., Worthen,A.J., Hirasaki, G.J., Nguyen,Q.P., Johnston,Keith.P. Ethoxylated Cationic Surfactants for CO₂ EOR in High Temperature, High Salinity Reservoirs. In: *the SPE Improved Oil Recovery Symposium*, Tulsa, Oklahoma, USA, 2012.
102. Spirov P., Rudyk S.N., Khan A.A. Foam Assisted WAG, Snorre Revisit with New Foam Screening Model. In: *the North Africa Technical Conference and Exhibition*, Cairo, Egypt, 2012.
103. Nikolov, A. D. , Wasan, D. T. , Huang, D. W. , Edwards, D. A. The Effect of Oil on Foam Stability: Mechanisms and Implications for Oil Displacement by Foam in Porous Media. In: *the SPE Annual Technical Conference and Exhibition*, New Orleans, Louisiana, 1986.
104. Yekeen, N., Manan, M. A., Idris, A. K., Padmanabhan, E., Junin, R. , Samin, A. M., Gbadamosi, A.O., Oguamah,I. A comprehensive review of experimental studies of nanoparticles-stabilized foam for enhanced oil recovery. *Petrol. J. Sci. Eng.*, 2018,164: 43–74.
105. Binks B.P., Lumsdon S.O., Influence of particle wettability on the type and stability of surfactant-free emulsions. *Langmuir*, 2000,16(23): 8622–8631.
106. Kumar S., Mandal A. Investigation on stabilization of CO₂ foam by ionic and nonionic surfactants in presence of different additives for application in enhanced oil recovery. *Appl. Surf. Sci.*, 2017,420: 9–20.
107. AlYousef Z., Almobarky M., Schechter D.S. Enhancing the stability of foam by the use of nanoparticles. *Energy Fuels*. 2017,31(10): 10620–10627.
108. Fameau A. L., Salonen A., Effect of particles and aggregated structures on the foam stability and aging. *Compt. Rendus Phys.*, 2014,15(8-9): 748–760.
109. Horozov T.S. Foams and foam films stabilised by solid particles. *Curr. Opin. Colloid Interface Sci.*, 2008,13(3): 134–140.
110. Sethumadhavan G.N., Nikolov A.D., Wasan D.T. Stability of liquid films containing monodisperse colloidal particles. *Colloid Interface Sci.*, 2001,240(1): 105–112.
111. Hunter, T. N. , Pugh, R. J. , Franks, G. V. , & Jameson, G. J. The role of particles in stabilising foams and emulsions. *Adv. Colloid Interface Sci.*, 2008,137(2): 57–81.
112. Farhadi, H. , Riahi, S. , Ayatollahi, S. , & Ahmadi, H. Experimental study of nanoparticle-surfactant-stabilized CO₂ foam: stability and mobility control. *Chem. Eng. Res. Des.*, 2016,111: 449–460.
113. Li, Z. , Wang, P. , Li, S. , Sun, Q. , Li, Y. Advances of researches on improving the stability of CO₂ foams by nanoparticles. *Journal of Southwest Petroleum University:ence & Technology Edition*,2014,36(4): 155–161.
114. [114]. Hosseini, H., Tsau, J. S., & Ghahfarokhi, R. B. Sub-millimetric visualization and stability measurement for supercritical CO₂ foams: Effect of ionic complexation on tubular and diverging flows. *Colloids and Surfaces A: Physicochemical and Engineering Aspects*, 2022,653, 129988.
115. Hosseini, H., Guo, F., Barati Ghahfarokhi, R., & Aryana, S. A. Microfluidic fabrication techniques for high-pressure testing of microscale supercritical CO₂ foam transport in fractured unconventional reservoirs. *Journal of Visualized Experiments*, 2020, 161:1-18.

116. Ettinger R. A., Radke C. J., The Influence of Texture on Steady Foam Flow in Berea Sandstone. *SPE Res. Eng.*,1992,7 (1): 83–90.
117. Falls A. H., Musters J. J., Ratulowski J. The Apparent Viscosity of Foams in Homogeneous Bead Packs. *SPE Res. Eng.*, 1989,4 (2): 155–164.
118. Ashoori E., Marchesin D., Rossen W. R., Roles of transient and local equilibrium foam behavior in porous media: Traveling wave. *Colloids & Surfaces A Physicochemical & Engineering Aspects*, 2011, 377(1-3): 228-242.
119. Davis, M. , Hille, E. , McDonnell, J., Mearns, D.F. In Basic physics of foam stability and collapse, *US NAVAIR*, 2012.
120. Bernard G. G., Jacobs W. L., Effect of Foam on Trapped Gas Saturation and on Permeability of Porous Media to Water. *SPE J.*, 1965,5(4): 295-300.
121. Kornev, K. G. , Neimark, A. V. , Rozhkov, A. N. Physical mechanisms of foam flow in porous media. *Rheology Series*, 1999, 8(99): 1151-1182.
122. Bowden F.P., Tabor,D. The Friction and Lubrication of Solids. *Department of Physical Chemistry, Cambridge University, England. Oxford University Press*, London, 1951, 19(7): 428.
123. Ren,G.W. Dynamics of Supercritical CO₂ Foam In Porous Media With CO₂ Soluble Surfactuants. *Dissertation*,The University of Texas at Austin,2012.
124. Rossen, W. , Zeilinger, S. , Shi, J., Lim, M. Simplified mechanistic simulation of foam processes in porous media. *SPE J.*, 1999, 4(3): 279-287.
125. Balan H. O., Balhoff M. T., Nguyen Q. P., Rossen, W. R. Network modeling of gas trapping and mobility in foam enhanced oil recovery. *Energy & Fuels*, 2011, 25(9): 3974-3987.
126. Shi J. X., Rossen W. R., Simulation and Dimensional Analysis of Foam Processes in Porous Media. In: *the Permian Basin Oil and Gas Recovery Conference*, Midland, Texas,1996.
127. Wang, F. , Li, Z. , Chen, H. , Lv, Q. , Silagi, W. , Chen, Z. Fractal characterization of dynamic structure of foam transport in porous media. *Journal of Molecular Liquids*, 2017, 241: 675-683.
128. Chou S. I., Percolation theory of foam in porous media. In: *the SPE/DOE Enhanced Oil Recovery Symposium*, Tulsa, Oklahoma,1990.
129. Lotfollahi, M. , Farajzadeh, R. , Delshad, M. , Varavei, A. ,Rossen, W. R.. Comparison of Implicit-Texture and Population-Balance Foam Models. *Journal of Natural Gas Science and Engineering*, 2016, 31:184-197.
130. CMG STARS User's Guid, version 2008.
131. Liu J., High-Resolution Methods for Enhanced Oil Recovery Simulations. *Dissertation*, The University of Texas at Austin,1993.
132. Chang Y.B., Lim M. T., Pope G. A., Sepehrnoori,K. CO₂ Flow Patterns Under Multiphase Flow. Heterogeneous Field Scale Conditions. *SPE Res.Eng.*, 1994,9 (3): 208–216.
133. Rossen W. R., Zhou Z. H. Modeling Foam Mobility at the Limiting Capillary Pressure. *SPE Advanced Technology Series* 1995,3 (1): 146–153.
134. Zhou Z. H., Rossen W. R. Applying Fractional-Flow Theory to Foam Processes at the 'Limiting Capillary Pressure'. *SPE Advanced Technology Series*,1995,3 (1): 154–162.
135. Fisher A. W., Foulser R. W. S., Goodyear S. G., Mathematical Modeling of Foam Flooding. In: *the SPE/DOE Enhanced Oil Recovery Symposium*, Tulsa, Oklahoma, 1990: 22–25.
136. Chang S. H., Grigg R. B. Effects of Foam Quality and Flow Rate on CO₂-Foam Behavior at Reservoir Conditions.In: *the SPE/DOE Improved Oil Recovery Symposium*, Tulsa, Oklahoma, 1998:19-22.
137. Shi J. X., Rossen W. R.Simulation of Gravity Override in Foam Processes in Porous media[J]. *SPE Res. Eval. & Eng.*, 1998,1(2): 148–154.
138. Jose M. A. M. Foam Flow Behavior in Porous Media: Effects of Flow Regime and Porous Media Heterogeneity. *Dissertation*,University of Texas-At Austin, 1998.
139. Rossen W. R., Wang M. W. Modeling Foams for Matrix Acid Diversion. In: *the SPE European Formation Damage Conference*, The Hague, Netherlands, 1997: 2-3.
140. Kovscek A. R., Patzek T. W., Radke C. J.Mechanistic Foam Flow Simulation in Heterogeneous and Multidimensional Porous Media. *SPE J.*,1997,2(4): 511-526.
141. Cheng L., Reme A. B., Shan D., Coombe,D.A., Rossen,W. R. Simulating Foam Processes at High and Low Foam Qualities.In: *the SPE/DOE Improved Oil Recovery Symposium*, Tulsa, Oklahoma, 2000: 3-5.
142. Bertin H. J., Foam Diversion Modeling Using a Bubble-Population Correlation.In:*the SPE/DOE Improved Oil Recovery Symposium*, Tulsa, Oklahoma, 2000: 3-5.
143. Kovscek A. R., Patzek T., Radke C. J., A mechanistic population balance model for transient and steady-state foam flow in Boise sandstone.*Chemical Engineering Science*,1995,50(23): 3783-3799.
144. Bertin H. J., Quitard M. Y., Castanier L. M. Development of a Bubble-Population Correlation for Foam-Flow Modeling on Porous Media. *SPE J.*, 1998,3 (4): 356-362.
145. Bertin H. J., Quitard M. Y., Castanier L. M., Modeling Foam Flow in Porous Media Using a Bubble Population Correlation. In:*SPE Annual Technical Conference and Exhibition*, New Orleans, Louisiana,1998
146. Li B., Hirasaki G. J., Miller C. A. Upscaling of Foam Mobility Control to Three Dimensions. In: *the SPE/DOE Symposium on Improved Oil Recovery*, Tulsa, Oklahoma, USA, 2006,22-26.

147. Chen Q., Gerritsen M. G., Kovscek A. R. Modeling Foam Displacement with the Local Equilibrium Approximation: Theory and Experiment Verification. In: *the SPE Annual Technical Conference and Exhibition, Denver, Colorado, USA, September 2008*: 21-24.
148. Radke C. J., Gillis J. V., A dual gas tracer technique for determining trapped gas saturation during steady foam flow in porous media. In: *Proceedings of the SPE Annual Technical Conf. and Exhibition*. 1990: 23–26.
149. Pang Z.X., Lv,X.C., Zhang,F.Y., Wu,T.T.,Gao,Z.N.,Geng,Z.G.,Luo,C.D. The macroscopic and microscopic analysis on the performance of steam foams during thermal recovery in heavy oil reservoirs. *Fuel*, 2018, 233: 166-176.
150. Rossen W. R., Foam Generation at Layer Boundaries in Porous Media. *SPE J.*, 1999,4(4): 409-412.
151. Kovscek A. R., Bertin H. J. Estimation of Foam Mobility in Heterogeneous Porous Media. In: *the SPE/DOE Improved Oil Recovery Symposium*, Tulsa, Oklahoma, 2002.
152. Shi J. X., Rossen W. R., Improved Surfactant-Alternating-Gas Foam Process to Control Gravity Override. In: *the SPE/DOE Improved Oil Recovery Symposium*, Tulsa, Oklahoma, 1998.
153. Doorwar S., Mohanty K. K., Pore-scale fingering during viscous oil displacement. In: *Proceedings of the International Symposium of the Society of Core Analysts*. Austin, 2011: 18-21.
154. Ayirala S. C. Surfactant-induced Relative Permeability Modifications for Oil Recovery Enhancement (M.Sc. thesis). *Dissertation,Louisiana State University*,2002.
155. Rao D. Gas injection EOR—a new meaning in the new millennium. *Can. Pet. Technol.* 2001,40(2): 11–18.
156. Srivastava M., Foam Assisted Low Interfacial Tension Enhanced Oil Recovery. *Dissertation*,the University of Texas Austin,2010.
157. Farajzadeh, R., Salimi, H., Zitha, P., Bruining, J. Numerical simulation of density-driven natural convection in porous media with application for CO₂ injection projects. In: *Proceedings of the SPE-EUROPEC/EAGE Conference*, 2007: 11–14.
158. Aleidan A. A., Mamora D. D., SWACO₂ and WACO₂ efficiency improvement in carbonate cores by lowering water salinity. In: *Proceedings of the Canadian Unconventional Resources and International Petroleum Conference*,2010: 19-21.
159. Denkov N. D. Mechanisms of action of mixed solid–liquid antifoams. 2. Stability of oil bridges in foam films. *Langmuir*. 1999,15(24): 8530-8542.
160. Ahmadi M., Chen Z., Challenges and future of chemical assisted heavy oil recovery processes. *Advances in Colloid and Interface Science*, 2019,275: 102081.
161. Xing, D. , Bing, W. , Mclendon, W. J. , Enick, R. M. , Soong, Y. CO₂-Soluble, Nonionic, Water-Soluble Surfactants That Stabilize CO₂-in-Brine Foams. *SPE J.*, 2012,17(4):1172 -1185.
162. Ramadhan,G.B. The Foaming Behavior of a CO₂-soluble, Viscoelastic Diamine Surfactant in Porous Media. *Dissertation*,the University of Texas at Austin,2018.
163. Liebum.,M.M. Characterization of an Alkyl Diamine Surfactant for Gas Mobility Control in Gas Enhanced Oil Recovery and Conformance Control. The University of Texas at Austin. 2016.
164. Eckert, C. A. , Debenedetti, P. G. , & Knutson, B. L. Supercritical fluids as solvents for chemical and materials processing. *Nature*, 1996, 383: 313-318.
165. AlYousef Z., Gizzatov A., Almajid M., Alabdulwahab A. Rheology, Stability, and Adsorption of an Amphoteric Foaming Agent for CO₂ Mobility Control Applications under Reservoir Conditions. *European Association of Geoscientists & Engineers*,2021.
166. Beckman E. J. A challenge for green chemistry: Designing molecules that readily dissolve in carbon dioxide. *Chemical communications*, 2004, 35(17): 1885-1888.
167. Sarbu T., Styranec T., Beckman E. J., Non-fluorous polymers with very high solubility in supercritical CO₂ down to low pressures. *Nature*. 2000, 405(6783): 165-168.
168. Ren G., Sanders A., Nguyen Q., New Method for the Determination of Surfactant Solubility and Partitioning Between CO₂ and Brine. *Journal of Supercritical Fluids*, 2014,91: 77-83.
169. Eastoe, J. , Dupont, A. , Paul, A. , Steytler, D. C. , & Rumsey, E. Design and Performance of Surfactants for Carbon Dioxide. *Supercritical Carbon Dioxide; ACS Symposium Series*,2003,19: 285-308.
170. Upadhyaya, A., Acosta, E. J., Scaemhorn, J. F., & Sabatini, D. A. Microemulsion phase behavior of anionic-cationic surfactant mixtures: Effect of tail branching. *Journal of Surfactants and Detergents*,2006,9: 169-179.
171. Gland, N., Chevallier, E., Cuenca, A., & Batot,G. New Developement of Cationic Surfactant Formulations for Foam Assisted CO₂-EOR in Carbonates Formations. In:*Abu Dhabi International Petroleum Exhibition & Conference*, 2018:12–15.
172. Sagisaka, M. , Koike, D. , Mashimo, Y. , Yoda, S. , Takebayashi, Y. , Furuya, T., Yoshizawa,A., Sakai,H., Abe,M., Otake,K. Water/Supercritical CO₂ Microemulsions with Mixed Surfactant Systems. *Langmuir*, 2008,24: 10116-10122.
173. Zhang, X. , Zhang, T. , Ge, J. , Wang, Y. , Zhang, G. . The CO₂-in-water foam stabilized with the mixture of CO₂-soluble surfactant and nonionic surfactant. *Journal of Petroleum Science and Engineering*,2020, 198(2): 108117.

174. Adkins, S. S.; Chen, X.; Nguyen, Q. P.; Sanders, A. W.; Johnston, K. P., Effect of branching on the interfacial properties of nonionic hydrocarbon surfactants at the air–water and carbon dioxide–water interfaces. *Journal of Colloid and Interface Science*, 2010, 346 (2):455-463.
175. Rosen M. J. In *Surfactants and Interfacial Phenomena*; 3rd Edition; John Wiley & Sons, Inc.: New York, 2004.
176. Rosen M. J., Kunjappu J. T., *Surfactants and Interfacial Phenomena*; Fourth Edition; John Wiley & Sons, Inc.: Hoboken, NJ, 2012.
177. McIlendon, W. J. , Koronaios, P. , McNulty, S. , Enick, R. M. , Biesmans, G. , Miller, A. N. Assessment of CO₂-Soluble Surfactants for Mobility Reduction using Mobility Measurements and CT Imaging. *Journal of Petroleum Science & Engineering*, 2014,119(3):196-209.
178. Gupta R. B., Shim J., Solubility in supercritical carbon dioxide. NW, CRC Press,2007.
179. Føyen T., Alcorn, Z. P. , Fern, M. A. , Barrabino, A. , Holt, T. CO₂ mobility reduction using foam stabilized by CO₂-and water-soluble surfactants. *Journal of Petroleum Science and Engineering*. 2021,196 (8):107651.
180. Ma K., Cui,L.Y, Dong Y. Wang,T.L.,Da Ch, Hirasaki,G.J., Biswal,S.L. Adsorption of Cationic and Anionic Surfactants on Natural and Synthetic Carbonate Materials. *Colloid Interf. Sci.*, 2013,408(15): 164–172.
181. Somasundaran P., Ananthapadmanabhan K. P., Celik M. S., Manev,E.D. A Thermodynamic Model of Redissolution of Calcium Sulfonate Precipitates in NaCl Solutions. *SPE J.*,1984,24(6): 667–676.
182. Christine Noïk, Marc Bavière, Daniel Defives. Anionic Surfactant Precipitation in Hard Water. *Colloid Interf. Sci.*, 1987,115(1): 36–45.
183. George G. Bernard, L. W. Holm, Craig P. Harvey. Use of Surfactant to Reduce CO₂ Mobility in Oil Displacement. *SPE J.*, 1980, 20(04): 281-292.
184. Zheng, X., Foster, E. , Wang, Y. , Nayak, S., Johnston, K. P. Effect of Grafted Copolymer Composition on Iron Oxide Nanoparticle Stability and Transport in Porous Media at High Salinity. *Energy & Fuels*. 2014, 28(6): 3655- 3665.
185. Levitt, D. , Jackson, A. , Heinson, C. , Britton, L. N. , Malik, T. ,Dwarakanath , Pope,G.A. Identification and Evaluation of High-Performance EOR Surfactants. *SPE Res. Eval. & Eng.* 2009, 12(02): 243-253.
186. Chen,Y., Elhag,A.,Poon,B., Cui,L.Y., Ma, K.,Liao,S.Y.,Reddy,P.P., Worthen,A.J.,Hirasaki,G.J.,Nguyen,Q.P., Biswal, S. L., Johnston, K.P. Switchable Nonionic to Cationic Ethoxylated Amine Surfactants for CO₂ Enhanced Oil Recovery in High-Temperature, High-Salinity Carbonate Reservoirs. *SPE J.* 2014. 19(2): 249–259. SPE-154222-PA.
187. Cui L., Ma, K. , Abdala, A. A. , Lu, J. , Tanakov, I. M. , Biswal, S. L., Hirasaki, G.J. Adsorption of a Switchable Cationic Surfactant on Natural Carbonate Minerals. *SPE J.*, 2014, 20(1): 70–78.
188. Cui, L. , Khramov, D. M. , Bielawski, C. W. , Hunter, D. L. , Paul, D. R. Effect of organoclay purity and degradation on nanocomposite performance, Part 1: Surfactant degradation. *Polymer*,2008, 49(17): 3751-3761.
189. Xie, W. , Gao, Z. , Pan, W. P. , Hunter, D. , Singh, A. , Vaia, R. Thermal Degradation Chemistry of Alkyl Quaternary Ammonium Montmorillonite. *Chem. Mater.*, 2001, 13(9): 2979-2990.
190. Chen, Y. , Elhag, A. S. , Worthen, A. J. , Reddy, P. P. , Ou, A. M. , Hirasaki, G. J., Nguyen Q.P.,Biswal, S.L., Johnston K P. High Temperature CO₂-in-Water Foams Stabilized with Cationic Quaternary Ammonium Surfactants. *J. Chem. Eng. Data.*, 2016,61(8): 2761–2770.
191. Zhou, J. , Srivastava, M., Hahn, R., Inouye, A.,Dwarakanath,V. Evaluation of an Amphoteric Surfactant for CO₂ Foam Applications: A Comparative Study. In: *the SPE Improved Oil Recovery Conference, Virtual, August 2020*.
192. Marcio T., Teresa C., A Gil, S. , Macedo, A. L. , Cabrita, E. J. , Ana, A. R. Molecular interactions and CO₂-philicity in supercritical CO₂. A high-pressure NMR and molecular modeling study of a perfluorinated polymer in scCO₂. *J.Phys.Chem. B.*, 2007, 111(6): 1318-1326.
193. Eastoe J., Cazelles B. M. H., Steytler D. C., Holmes, J. D., Heenan, R. K. Water-in-CO₂ microemulsions studied by small-angle neutron scattering. *Langmuir*, 1997, 13(26): 6980-6984.
194. Eastoe J., Paul A., Downer A., Steytler,D.C., Rumsey,E. Effects of fluorocarbon surfactant chain structure on stability of water-in-carbon dioxide microemulsions. Links between aqueous surface tension and microemulsion stability. *Langmuir*, 2002, 18(8): 3014-3017.
195. Li,Z.M.,Xi,L.H.,Zhang,C.,Wang,M.J.Progress of Reducing Miscibility Pressure between CO₂ and Crude Oil by CO₂-soluble Surfactant. *Oilfield Chemistry*,2020, 37(4): 745-751.
196. Fink R., Hancu D., Valentine R., Beckman E J. Toward the development of “CO₂-philic” hydrocarbons. 1. Use of side-chain functionalization to lower the miscibility pressure of polydimethylsiloxanes in CO₂. *J. Phys. Chem. B.*, 1999, 103(31): 6441-6444.
197. Fink R., Beckman E. J., Phase behavior of siloxane-based amphiphiles in supercritical carbon dioxide. *J. Supercrit. Fluids*, 2000, 18(2): 101-110.
198. Memon M., Shuker M., Elraies K., Study of blended surfactants to generate stable foam in presence of crude oil for gas mobility control. *Journal of Petroleum Exploration and Production Technology*, 2016, 7:77-85.

Disclaimer/Publisher's Note: The statements, opinions and data contained in all publications are solely those of the individual author(s) and contributor(s) and not of MDPI and/or the editor(s). MDPI and/or the editor(s) disclaim responsibility for any injury to people or property resulting from any ideas, methods, instructions or products referred to in the content.